The University of Melbourne

Department of Mathematics and Statistics

The Wiener-Hopf Method and Its Applications in Fluids

Juwen Ho

Supervisor : Associate Professor John Sader

Applied Mathematics

Honours Thesis

November 28, 2007

Acknowledgements

I would like to thank my supervisor John Sader for giving me the opportunity to explore the very interesting world of fluids. His encouragement, passion and patience has proven to be invaluable to me throughout the year. A special thanks to Assoc. Prof. Barry Hughes and Paul Pearce for helping me with the numerous questions I have in complex analysis.

Thank you to the other Honours students in G69 for making this year a more enjoyable one and a year to treasure.

Contents

Chapter 1

Introduction

The geometry of an object submerged in fluid and its interactions with the fluid has long been an open area of research. Since the time of Stokes, who studied the flow of a viscous fluid around a sphere, it was perceived that the structure of the object in the fluid is important. Demonstrated by his study on spheres in fluid, Stokes came up with the well known formula of the drag force on a sphere, which includes variables that are linked to the geometry of the sphere.

Flat plates or blades in fluids have been studied since the time of Blasius and used considerably throughout the scientific community particularly in engineering. These plates have been implemented to design better and smaller diagnostic tools and to be able to measure some physical quantity such as density or viscosity of a fluid. Such devices can be made in the order of microns, which is sometimes lumped into the category of a micro-electrical mechanical system (MEMS) or even to the scale of nanometres and categorized as a nano-electrical mechanical system (NEMS). Arguably, the atomic force microscope (AFM), which is a device which consists of a clamped cantilever beam with a weighted tip at the free end, has been seen as one of the greatest uses of plates/blades. Not only is it be able to measure physical quantities, but it can also provide information about the surface of a material down to nanometre resolution, for testing of nanomaterials and the list goes on. Typically, the AFM undergoes oscillations in fluid and therefore understanding how the fluid and the cantilever interact is important to ensure accuracy and precision when measuring.

Quite a number of people have modelled the AFM cantilever immersed in an inviscid fluid, that is, a fluid having no viscosity. But, even though most regions of the problem can be modeled by an inviscid fluid, viscous effects are significant and penetrate a small distance away from its surface. As length scales decrease, viscous effects cannot be neglected since the thickness of the viscous penetration depth becomes comparable with the length scale. This is especially true when modelling small objects such as the AFM cantilever and thus we must consider viscous effects on the cantilever.

It is known from the study of semi-infinite plates in a two dimensional viscous fluid flow that the edge of a plate is of particular importance. The edge of a blade gives a significant contribution due to viscous effects that may be different from regions far away from the edge. Thus, a blade with 2 edges would be make it all the more important to be able to account for the viscous effects and subsequently the fluid's effect on the blade. Since we are considering blades with very large aspect ratio where the length greatly exceeds the width, we need to account for the edges at the sides of the blade only, since it can be approximated by a blade with infinite *length* and finite width.

Tuck [17] has done a numerical analysis on a blade with negligible thickness oscillating parallel to its surface orientation by solving integral equations. He found that the coefficient due to the damping force as the blade oscillates behaves like $C/\sqrt{\beta} \sim 3.2/\sqrt{\beta}$, where β is the Reynolds number associated with this problem. The Reynolds number used in Tuck's analysis was

$$\beta = \frac{\rho \omega L^2}{4\mu} \quad ,$$

where ρ and μ are the density and the viscosity of the fluid and L is the length of the blade. He proposed that to obtain a first non-zero damping coefficient to correct for the potential (or inviscid) flow, one would have to carry out an asymptotic expansion for large β. The method he proposed to use was the Wiener-Hopf technique to be able to obtain the damping coefficient.

Recently, Atkinson and de Lara [3] have used the Wiener-Hopf method to solve a fluid flow problem on an oscillating plate that is similiar to the problem considered by Tuck. Their problem consists of an infinitely *wide* plate but finite length, clamped at one end and the free end undergoes oscillations. They have also solved the problem of a flat disk vibrating in a viscous fluid [2]. Armed with this knowledge we can apply their methodology to carry out the analysis suggested by Tuck.

In Chapter 2 of this thesis, the Wiener-Hopf method is discussed and in particular how to decompose functions since it is the crux of the method. Chapter 3 focuses on expounding Atkinson and de Lara's analysis, which will serve as the basis for the other problems considered here. In Chapter 4, the Wiener-Hopf method is applied again to the problem considered by Tuck and a problem where the blade undergoes torsional oscillations about the middle of the blade. The forces and moments experienced by the blade are calculated and the hydrodynamic function is obtained. This function will give the damping coefficient to be able to compare with results from Tuck.

In Chapter 5, the forces and moments obtained in the previous chapter are compared with their corresponding exact solutions obtained by Van Eysden and Sader [6]. A comparison is also made with the findings of Sader [15] for the problem of Tuck and the findings of Green and Sader [7] for the problem of torsional oscillations of a blade.

Chapter 2

The Wiener-Hopf Technique

The Wiener-Hopf technique was originally formulated to solve certain classes of integral equations. Since then, this technique has been widely used to solve certain types of partial differential equations (PDEs) particularly particularly mixed boundary value problems. This has been proven very useful use when solving radiation or diffraction problems [13] where there are obstacles that generate reflected and transmitted waves [9]. It is also quite closely related to the Riemann-Hilbert problem. In this chapter, we shall review the main ideas on how to solve problems using this technique.

2.1 The Wiener-Hopf Method

Suppose we have a boundary value problem with a PDE and the boundary conditions (BCs) are specified only on the semi-infinite domain. The problem can be either the half plane or the whole of $\mathbb{R}^2$ and the boundary data is typically given on the real line. An example would be the Laplace equation on the upper half plane.

$$\nabla^2\phi = 0$$

$$\text{BCs:} \begin{cases} \phi = 0, & y = 0 \text{ and } x > 0 \\ \frac{\partial\phi}{\partial y} = 0, & y = 0 \text{ and } x < 0 \end{cases}$$

We typically apply Fourier transforms to the PDE and its boundary conditions and we assume that we can solve the Fourier transformed equation. The Fourier transform of the spatial variable, x, used throughout this thesis is defined as

$$\overline{F}(\zeta) = \int_{-\infty}^{\infty} f(x)e^{i\zeta x}\mathrm{d}x \quad .$$

Because the boundary conditions are specified over the semi-infinite domain, we would normally find that there will be two unknown functions corresponding to the unspecified part of the domain in the BCs. One would be analytic in the upper half plane ($Im(\zeta) > \tau_+$) and we shall call this a plus function. The other would be analytic in the lower half plane ($Im(\zeta) < \tau_-$) and we shall call this a minus function. After applying the Fourier transformed boundary conditions to the PDE, we would typically get an equation of the form

$$\overline{\phi_+}(\zeta) = \frac{\overline{\psi_-}(\zeta)}{A(\zeta)} + B(\zeta) \quad , \tag{2.1}$$

where $\overline{\phi_+}$ and $\overline{\psi_-}$ are the unknown functions.

This equation has a common region of analyticity if $\tau_+ < Im(\zeta) < \tau_-$ (see Fig. 2.1). In the most strict case, this analytic strip would only be a line and we can view this as the limit as $\tau_- \to 0^+$ and $\tau_+ \to 0^-$, where τ_- approaches 0 from above and τ_+ approaches 0 from below. We will now

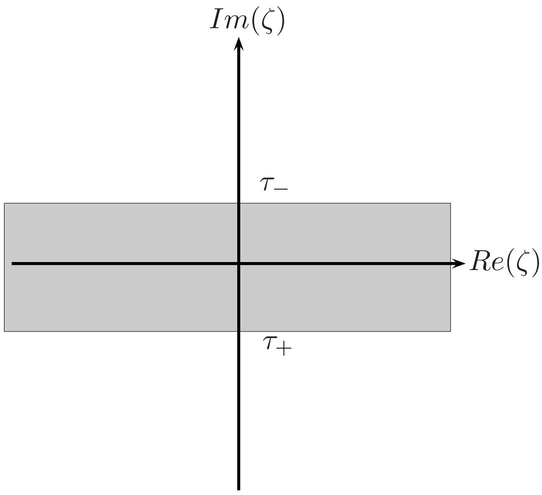

Figure 2.1: The shaded area represents the strip where the (2.1) is defined

want to perform a product decomposition of the form

$$A(\zeta) = A_-(\zeta)A_+(\zeta) \quad , \tag{2.2}$$

where $A_-(\zeta)$ is analytic in the lower half plane and $A_+(\zeta)$ is analytic in the upper half plane. Substituting (2.2) and multiplying both sides of equation (2.1) by $A_+(\zeta)$, we obtain

$$A_+(\zeta)\overline{\phi_+}(\zeta) = \frac{\overline{\psi_-}(\zeta)}{A_-(\zeta)} + B(\zeta)A_+(\zeta) \quad . \tag{2.3}$$

We perform another decomposition on the function $B(\zeta)A_+(\zeta)$ into a sum of two functions, i.e.

$$B(\zeta)A_+(\zeta) = C_+(\zeta) + C_-(\zeta) \quad . \tag{2.4}$$

As usual, $C_-(\zeta)$ is analytic in the lower half plane and $C_+(\zeta)$ is analytic in the upper half plane. Substituting (2.4) into (2.3) and rearranging the terms so that the plus functions are on one side of the equation and the minus functions are on the other side of the equation to give

$$A_+(\zeta)\phi_+(\zeta) - C_+(\zeta) = \frac{\psi_-(\zeta)}{A_-(\zeta)} + C_-(\zeta) \equiv G(\zeta) \quad , \tag{2.5}$$

where $G(\zeta)$ is defined as as above. The equation that is defined by $G(\zeta)$ is analytic in the strip $\tau_+ < Im(\zeta) < \tau_-$. But the first part of (2.5) is analytic in the upper half plane and the second part of the equation is analytic in the lower half plane. Therefore, by analytic continuation, we can conclude that the function $G(\zeta)$ is analytic over the whole complex plane. Suppose that we can show that

$$\begin{aligned} |A_+(\zeta)\overline{\phi_+}(\zeta) - C_+(\zeta)| < |\zeta|^p \quad \text{as} \quad |\zeta| \to \infty, \quad Im(\zeta) > \tau_- \quad , \\ \left| \frac{\overline{\psi_-}(\zeta)}{A_-(\zeta)} + C_-(\zeta) \right| < |\zeta|^q \quad \text{as} \quad |\zeta| \to \infty, \quad Im(\zeta) < \tau_+ \quad . \end{aligned}$$

Then by the generalised Liouville's theorem, the function $G(\zeta)$ is a polynomial $P(\zeta)$ of degree less than equal to the intergral part of $min(p, q)$. Therefore we can solve for the two functions $\phi_+(\zeta)$ and $\psi_-(\zeta)$ separately, i.e.

$$\begin{aligned} \overline{\phi_+}(\zeta) &= \frac{P(\zeta) + C_+(\zeta)}{A_+(\zeta)} \quad , \\ \overline{\psi_-}(\zeta) &= A_-(\zeta)\left(P(\zeta) - C_-(\zeta)\right) \quad . \end{aligned}$$

Upon solving the two unknown functions separately, we can now solve the original boundary value problem by taking inverse Fourier transforms.

2.2 Product Decomposition of $A(\zeta)$

In performing the Wiener-Hopf method, we need to decompose a function into a product of two functions, one analytic in the lower half plane and the

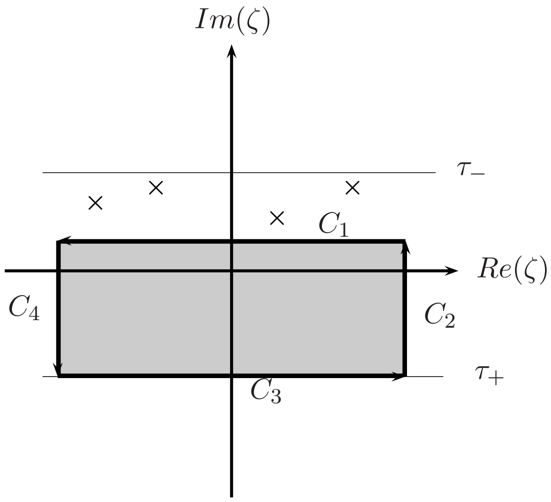

Figure 2.2: Contour integration for product decomposition. The crosses are the zeros of $H(\zeta)$

other in the upper half plane. In some simple cases, this can be done by inspection, but most of the time doing this decomposition is not immediately obvious. Here we shall see a general systematic way in performing this decomposition by using contour integration.

We will consider the function $A(\zeta)$ to be analytic in the strip $\tau_+ < Im(\zeta) < \tau_-$. We may also consider that the function may have some zeros inside the strip of analyticity as well. We shall choose a rectangular contour that is below all of the zeros inside the strip. This strip will also contain the inversion contour of the inverse Fourier transform since the contour can be anywhere within the analytic strip (see Fig. 2.2).

The function $A(\zeta)$ is analytic inside this rectangle comprises of the contours $\Gamma = C_1 + C_2 + C_3 + C_4$ and there are no zeros inside this rectangle. We also require that the function $A(\zeta) \to 1$ as $|\zeta| \to \infty$ to ensure that the contributions from C_2 and C_4 vanish as $|\zeta| \to \infty$. In order to express $A(\zeta)$

as a product $A_+(\zeta)A_-(\zeta)$, we take the logarithm of equation (2.2) to get

$$\ln(A(\zeta)) = \ln(A_+(\zeta)A_-(\zeta)) = \ln(A_+(\zeta)) + \ln(A_-(\zeta)) \quad .$$

We also note that $\ln(A(\zeta))$ is also analytic in the rectangle because it has no branch points since there are no zeros there, so we can apply the Cauchy integral formula.

$$\begin{aligned} \ln(A(\zeta)) &= \frac{1}{2\pi i}\int_\Gamma \frac{\ln(A(z))}{z-\zeta}\mathrm{d}z \\ &= \frac{1}{2\pi i}\left[\int_{C_1} \frac{\ln(A(z))}{z-\zeta}\mathrm{d}z + \int_{C_3} \frac{\ln(A(z))}{z-\zeta}\mathrm{d}z + \int_{C_3+C_4} \frac{\ln(A(z))}{z-\zeta}\mathrm{d}z\right] \quad . \end{aligned}$$

So far we have no guarantee that the contributions from the contours of C_2 and C_4 cancel out due to the multivaluedness of the logarithm as we go around the contour. We may have in the limit as $|\zeta| \to \infty$ that

$$\ln(A(\zeta)) \to \ln(e^{2\pi i n}) = 2\pi i n, \quad n \in \mathbb{Z} \quad .$$

But for the purposes of this thesis, we will only consider the case when $A(\zeta)$ is even and the inversion contour for the inverse Fourier transform on the real axis. It can be shown that given these conditions, the contributions from the contour C_2 and C_4 will cancel each other. For a more general method to deal with cases where the function is not even and not necessarily analytic on the real axis, we would refer to some texts regarding these types of decomposition [11]. Therefore we have

$$\ln(A_+(\zeta)) + \ln(A_-(\zeta)) = \frac{1}{2\pi i}\int_{C_1} \frac{\ln(A(z))}{z-\zeta}\mathrm{d}z + \frac{1}{2\pi i}\int_{C_3} \frac{\ln(A(z))}{z-\zeta}\mathrm{d}z \quad .$$

In the first integral, we may let ζ be anywhere below C_1 where C_1 is arbitrarily close to $Im(\zeta) = \tau_+$ from above. We can therefore conclude that that the integral

$$\frac{1}{2\pi i}\int_{C_1}\frac{\ln(A(z))}{z-\zeta}\mathrm{d}z, \quad Im(\zeta) < \tau_+$$

is analytic in the lower half plane and can be identified as a minus function. Similiarly for the second integral, we may let ζ be anywhere above C_3 where C_3 is arbitrarily close to $Im(\zeta) = \tau_+$ from above. We can now conclude that the integral

$$\frac{1}{2\pi i}\int_{C_3}\frac{\ln(A(z))}{z-\zeta}\mathrm{d}z, \quad Im(\zeta) > \tau_+$$

is analytic in the upper half plane and can be identified as a plus function. Since we have analyticity on the real axis, we therefore have that C_1 and C_3 on the real axis. So we now obtain the following expressions

$$\ln(A_+(\zeta)) = \frac{1}{2\pi i}\int_{-\infty}^{\infty}\frac{\ln(A(z))}{z-\zeta}\mathrm{d}z, \quad Im(\zeta) > 0 \tag{2.6}$$

$$\begin{aligned}\ln(A_-(\zeta)) &= -\frac{1}{2\pi i}\int_{\infty}^{-\infty}\frac{\ln(A(z))}{z-\zeta}\mathrm{d}z\\ &= -\frac{1}{2\pi i}\int_{-\infty}^{\infty}\frac{\ln(A(z))}{z-\zeta}\mathrm{d}z, \quad Im(\zeta) < 0\end{aligned} \tag{2.7}$$

Exponentiating equation (2.6) and (2.7) we obtain

$$\begin{aligned}A_+(\zeta) &= \exp\left(\frac{1}{2\pi i}\int_{-\infty}^{\infty}\frac{\ln(A(z))}{z-\zeta}\mathrm{d}z\right) \quad ,\\ A_-(\zeta) &= \exp\left(-\frac{1}{2\pi i}\int_{-\infty}^{\infty}\frac{\ln(A(z))}{z-\zeta}\mathrm{d}z\right) \quad .\end{aligned} \tag{2.8}$$

2.3 Sum Decomposition of $B(\zeta)A_+(\zeta)$

Similiarly for the sum decompostion, for some cases the decomposition can be done by inspection but most of the time it requires a more general approach by using contour integration again.

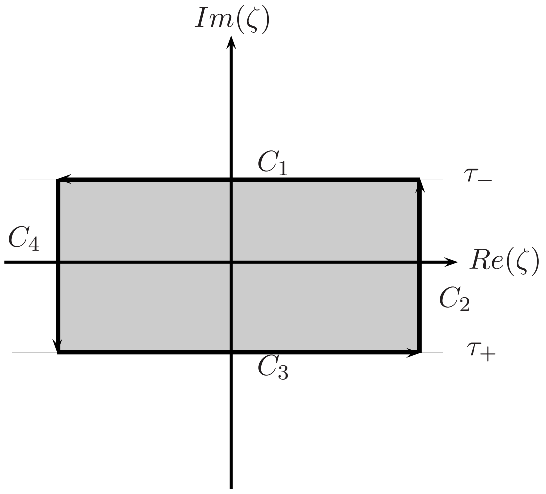

Figure 2.3: Contour integration for sum decomposition

We again have that $B(\zeta)A_+(\zeta)$ is analytic in the strip $\tau_+ < Im(\zeta) < \tau_-$ and so we can apply the Cauchy integral formula to obtain

$$B(\zeta)A_+(\zeta) = \frac{1}{2\pi i}\int_\Gamma \frac{B(z)A_+(z)}{z-\zeta}\mathrm{d}z \quad ,$$

where $\Gamma = C_1+C_2+C_3+C_4$ (see Fig. 2.3). We require that $|B(\zeta)A_+(\zeta)| \to 0$ so that the contributions of the contours C_2 and C_4 will vanish as $|\zeta| \to \infty$. Therefore, we have that

$$\begin{aligned} B(\zeta)A_+(\zeta) &= \frac{1}{2\pi i}\int_\Gamma \frac{B(z)A_+(z)}{z-\zeta}\mathrm{d}z \\ &= \frac{1}{2\pi i}\int_{C_1} \frac{B(z)A_+(z)}{z-\zeta}\mathrm{d}z + \frac{1}{2\pi i}\int_{C_3} \frac{B(z)A_+(z)}{z-\zeta}\mathrm{d}z \quad . \end{aligned} \tag{2.9}$$

The first integral in (2.9) is analytic for $Im(\zeta) < \tau_-$ and therefore a minus function while the second integral is analytic for $Im(\zeta) > \tau_+$ and therefore a plus function. Putting together this fact with (2.4), we get

$$\begin{aligned}
C_+(\zeta) &= \frac{1}{2\pi i}\int_{-\infty+i\tau_+}^{\infty+i\tau_+}\frac{B(z)A_+(z)}{z-\zeta}\mathrm{d}z \\
C_-(\zeta) &= \frac{1}{2\pi i}\int_{\infty+i\tau_-}^{-\infty+i\tau_-}\frac{B(z)A_+(z)}{z-\zeta}\mathrm{d}z \quad , \\
&= -\frac{1}{2\pi i}\int_{-\infty+i\tau_-}^{\infty+i\tau_-}\frac{B(z)A_+(z)}{z-\zeta}\mathrm{d}z \quad .
\end{aligned}$$

As before in the previous section, we will consider the case when $\tau_+ \to 0^-$ and $\tau_- \to 0^+$. Hence, we now obtain the expression for the sum decompositions as

$$\begin{aligned}
C_+(\zeta) &= \frac{1}{2\pi i}\int_{-\infty}^{\infty}\frac{B(z)A_+(z)}{z-\zeta}\mathrm{d}z, \quad Im(\zeta) > 0 \quad , \\
C_-(\zeta) &= -\frac{1}{2\pi i}\int_{-\infty}^{\infty}\frac{B(z)A_+(z)}{z-\zeta}\mathrm{d}z, \quad Im(\zeta) < 0 \quad .
\end{aligned} \tag{2.10}$$

Chapter 3

Oscillating Plate with Clamped End in Viscous Fluid

We will now review the method proposed by Atkinson and de Lara [3] to solve the problem of obtaining the frequency response on a rectangular plate oscilating in a viscous fluid. The model used here is a plate that has a length of L, a width of W and a thickness of T where it is assume that $T \ll L, W$ and $L \approx W$ or $L < W$. The plate is clamped along one edge while the other edges are free to vibrate at a frequency of ω (see Fig. 3.1). The motivation for using such a model was to design sensors to be able to measure fluid viscosity and density. This would be implemented in a MEMS where typically the length and the width are in the order of milimetres and the thickness is in the order of microns.

Since the model considered here is wider than it is long, the authors assumed that all longitudinal cross sections behave the same with negligible effects on the 2 parallel edges with the third edge having the dominant

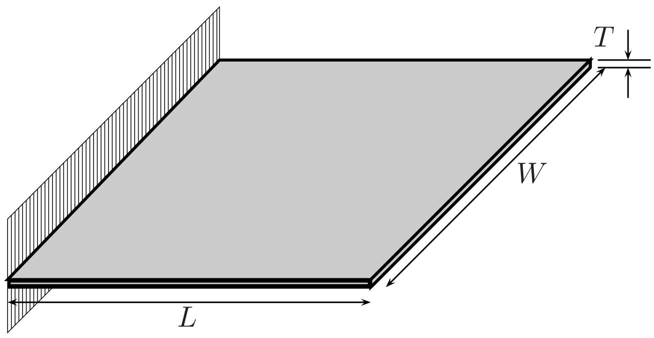

Figure 3.1: Plate clamped at one end with length L, width W and thickness T and $T \ll W, L$ and $L < W$

effect on the plate. In other words, they have considered an infinitely wide plate clamped on one edge and the other free to vibrate and thus giving the main contribution to the viscous fluid flow. Therefore, the 3-dimensional model can now be reduced to a problem involving planar flow along one longitudinal cross section.

The approach that was taken by Atkinson and de Lara was to solve for the fluid flow surrounding the plate and obtain the fluid pressure exerted on the vibrating plate. This is done in two steps: first, the case where the fluid is inviscid is solved and then obtain a correction to the inviscid solution by allowing viscous effects via the Wiener-Hopf technique mentioned in Chap. 2. This is thought of as the leading order in a matched asymptotic expansion between the region of inviscid flow and the region of viscoud flow near the surface. Once the fluid pressure is found, the equation of motion of the thin plate is solve by balancing the forces experienced by the plate.

3.1 Assumptions

6 main assumptions were made in describing the problem:

1. The width of the plate is far greater than the length of the plate.

2. The fluid is considered to be infinite with no wall effects.
3. The amplitude of oscillation is smaller than any length scale in the problem.
4. The fluid is incompressible with density ρ.
5. The thickness of the plate is negligible.
6. The fluid is Newtonian with a viscosity of μ.

Assumption 1 means that the dominant length scale in our problem is just the length L. A consequence of assumption 3 is that the non-linear convective term ($\mathbf{u} \cdot \nabla \mathbf{u}$) that appears in the Navier-Stokes equation which governs viscous fluid flow can now be removed. This is because $\mathbf{u} \sim amplitude$ and so, for sufficiently high frequencies but not too high such that the fluid becomes compressible,

$$O(amplitude) = \frac{\partial \mathbf{u}}{\partial t} \gg \mathbf{u} \cdot \nabla \mathbf{u} = O(amplitude^2) \quad .$$

From assumption 4, the continuity equation can also be reduced to a simpler form. For most practical purposes of modeling small mechanical systems, the fluid velocity doesn't exceed the speed of sound and the wave length of the speed of sound is far greater than the length L. We have assumption 5 so that we can use the theory of thin plates when solving for the equation of motion for the plate. Also, the effects of the fluid coming from the thickness of the plate are neglected. Therefore, the governing equation for this problem would be the linearized Navier-Stokes equations:

$$\begin{gathered} \rho \frac{\partial \mathbf{u}}{\partial t} = -\nabla p + \mu \nabla^2 \mathbf{u} \quad , \\ \nabla \cdot \mathbf{u} = 0 \quad . \end{gathered} \tag{3.1}$$

3.2 Scaling of Governing Equations

Since we are considering oscillations of the plate, it would be easier to work in terms of the Fourier transformed version of (3.1) where the Fourier transform of the time variable is

$$\tilde{X} = \int_{-\infty}^{\infty} X e^{i\omega t} \mathrm{d}t \quad .$$

Applying the Fourier transform to (3.1), we get

$$\begin{aligned} -i\omega\tilde{\mathbf{u}} &= -\nabla\tilde{p} + \mu\nabla^2\tilde{\mathbf{u}} \quad , \\ \nabla\cdot\tilde{\mathbf{u}} &= 0 \quad . \end{aligned} \tag{3.2}$$

From (3.2) we make all the variables dimensionless by defining $\tilde{p} = \omega\rho L U\hat{p}$, $\tilde{\mathbf{u}} = U\hat{\mathbf{u}}$ and the coordinates x, y and z are scaled by dividing by the length of the plate L. We also define a dimensionless quantity

$$\beta = \frac{\rho\omega L^2}{\mu} \quad ,$$

where this quantity is commonly known as the Reynolds number [4]. Although the Reynolds number is associated with the non-linear convective term, this is not the case here. The governing equation now becomes

$$-i\hat{\mathbf{u}} = -\hat{\nabla}\hat{p} + \frac{1}{\beta}\hat{\nabla}^2\hat{\mathbf{u}} \quad , \tag{3.3a}$$

$$\hat{\nabla}\cdot\hat{\mathbf{u}} = 0 \quad . \tag{3.3b}$$

From here on, we will drop the hatted signs for simplicity and note that all the results are presented in the frequency domain and that all variables are dimensionless.

3.3 Solving for the fluid reaction

3.3.1 Inviscid Solution

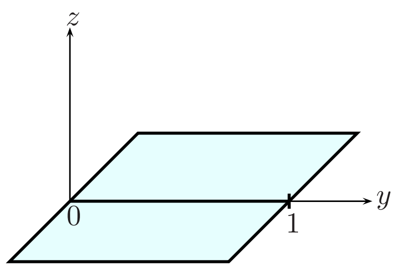

Figure 3.2: The plate representing by the line going from 0 (clamped end) to 1 (free end) in the scaled coordinate system

In the figure, the plate is located in the $z = 0$ plane along the y-axis between $y = 0$ (the clamped end) and $y = 1$ (the free end) (see Fig. 3.2). Using the assumptions stated in Sec. 3.1 together with the viscosity of the fluid being zero ($\beta \to \infty$), we set the velocity and the pressure of the inviscid fluid to be

$$\mathbf{u} = \nabla\phi \tag{3.4a}$$

$$p = i\phi \quad , \tag{3.4b}$$

where ϕ is the velocity potential so that $\nabla^2\phi = 0$. With this choice of $\mathbf{u}$ and p, it solves (3.3). We will also define the pressure differential $[p]$ about $z = 0$ as

$$[p] = p|_{z=0^+} - p|_{z=0^-} \quad . \tag{3.5}$$

The velocity potential satisfies Laplace's equation after substituting equation (3.4a) into (3.3b). Laplace's equation is given to be

$$\nabla^2\phi = 0 \quad .$$

Laplace's equation has the solution

$$\phi = \arctan(\frac{z}{y}) \quad .$$

If we shift our origin from $y = 0$ to $y = s$,

$$\phi = \arctan(\frac{z}{y-s})$$

is also a solution to Laplace's equation. Using superposition over s, we get the general solution for the velocity potential to be

$$\phi = \int_0^1 f(s) \arctan(\frac{z}{y-s}) \mathrm{d}s \quad , \tag{3.6}$$

where the function $f(s)$ is to be determined from the boundary conditions. We define the standard arctangent function to take the values

$$\arctan(\frac{z}{y-s}) = \begin{cases} \pi & \text{if } z = 0^+, y < s \\ 0 & \text{if } z = 0^+, y > s \\ -\pi & \text{if } z = 0^-, y < s \\ 0 & \text{if } z = 0^-, y > s \end{cases} \tag{3.7}$$

The boundary conditions are imposed on the plane $z = 0$ since that is where the plate is located.

- The vertical velocity, denoted by u_z is continuous everywhere and known for the plate as a function of y but unknown outside the plate

$$u_z|_{z=0^+} = u_z|_{z=0^-} = \begin{cases} \text{unknown function} & y < 0 \\ u_z(y) & 0 < y < 1 \\ \text{unknown function} & y > 1 \end{cases} \tag{3.8}$$

- The pressure differential is unknown for the plate but equal to zero outside the plate for $y > 1$. On the other side of the plate at $y < 0$, we do not expect the pressure differential to be zero but finite. This represents the clamping of the plate at $y = 0$

$$[p] = \begin{cases} \text{finite} & y < 0 \\ \text{unknown function to be determined} & 0 < y < 1 \\ 0 & y > 1 \end{cases} \tag{3.9}$$

Atkinson and de Lara quoted the additional condition that the tangential velocity, denoted by u_y is continuous and equal to zero at $z = 0$ for the inviscid solution. This condition is the no-slip boundary condition and is a condition only for the viscous case since inviscid fluids can have a non-zero tangential velocity and not a condition used to solve Laplace's equation. This, however, is used as a check for the inviscid solution on whether it is satisfied even though it is an inviscid fluid. We now have two boundary conditions for Laplace's equation and therefore we are able to solve it.

The vertical velocity can be obtained by differentiating (3.6) with respect to z:

$$u_z = \int_0^1 f(s) \frac{1}{\left(1 + (\frac{z}{y-s})^2\right)} \frac{1}{y - s} \mathrm{d}s \quad . \tag{3.10}$$

Applying the boundary condition (3.8) to (3.10), we get the singular integral equation

$$u_z(y) = \int_0^1 \frac{f(s)}{y-s}\mathrm{d}s, \quad 0 < y < 1 \tag{3.11}$$

where the integral is defined as a Cauchy principal value and subsequently all integrals are defined as Cauchy principal value. We refer to some texts [1, 11, 12] on obtaining the general solution of (3.11). This is given to be

$$\begin{aligned} f(s) &= \frac{1}{\pi^2\sqrt{s(1-s)}}\int_0^1 u_z(y')\frac{\sqrt{y'(1-y')}}{y'-s}\mathrm{d}y' + \frac{A}{\sqrt{s(1-s)}} \\ &= \frac{1}{\pi^2\sqrt{s(1-s)}}\int_0^1 u_z(y')\sqrt{\frac{1-y'}{y'}}(1+O(s))\mathrm{d}y' + \frac{A}{\sqrt{s(1-s)}} \\ &= \frac{1}{\pi^2\sqrt{s(1-s)}}\left(A + \frac{1}{\pi^2}\int_0^1 u_z(y')\sqrt{\frac{1-y'}{y'}}\mathrm{d}y'\right) + O(\sqrt{s}) \quad , \end{aligned} \tag{3.12}$$

where we have done a binomial expansion for small s in the integral. Applying the boundary condition (3.9) to (3.12) requires that at $s = 0$ the function $f(s)$ is finite and therefore the coefficient of the $1/\sqrt{s}$ has to be zero:

$$\begin{aligned} & A + \frac{1}{\pi^2}\int_0^1 u_z(y')\sqrt{\frac{1-y'}{y'}}\mathrm{d}y' = 0 \\ \Rightarrow \quad & A = -\frac{1}{\pi^2}\int_0^1 u_z(y')\sqrt{\frac{1-y'}{y'}}\mathrm{d}y' \quad . \end{aligned} \tag{3.13}$$

We can now re-write the function $f(s)$ to be

$$\begin{aligned} f(s) &= \frac{1}{\pi^2\sqrt{s(1-s)}}\int_0^1 u_z(y')\left(\frac{\sqrt{y'(1-y')}}{y'-s} - \sqrt{\frac{1-y'}{y'}}\right)\mathrm{d}y' \\ &= \frac{1}{\pi^2\sqrt{s(1-s)}}\int_0^1 u_z(y')\left(\frac{y'\sqrt{1-y'} - (y'-s)\sqrt{1-y'}}{\sqrt{y'}(y'-s)}\right)\mathrm{d}y' \\ &= \frac{1}{\pi^2}\sqrt{\frac{s}{1-s}}\int_0^1 \frac{u_z(y')}{y'-s}\sqrt{\frac{1-y'}{y'}}\mathrm{d}y' \quad . \end{aligned} \tag{3.14}$$

The function $f(s)$ has now been determined and we now proceed to finding an expression for the tangential velocity at $z = 0$. At $z = 0^+$ and $z = 0^-$, (3.6) becomes

$$\begin{aligned} \phi|_{z=0^+} &= \pi \int_y^1 f(s)\mathrm{d}s \\ \phi|_{z=0^-} &= -\pi \int_y^1 f(s)\mathrm{d}s \end{aligned} \tag{3.15}$$

by using the values of the arctangent specified in (3.7). By differentiating (3.15) with respect to y using (3.4a), we get the tangential velocity u_y at $z = 0^+$ to be

$$u_y = -\pi f(y) \quad .$$

We observe a singularity at the edge of the plate where it has the following leading order behaviour

$$\begin{aligned} u_y|_{y\to 1^-} &\approx -\frac{\pi}{\pi^2\sqrt{1-y}} \int_0^1 \frac{u_z(y')}{y'-1}\sqrt{\frac{1-y'}{y'}}\mathrm{d}y' \\ &= \frac{1}{\pi\sqrt{1-y}} \int_0^1 \frac{u_z(y')}{\sqrt{y'(1-y')}}\mathrm{d}y' \\ &= \frac{B}{\sqrt{1-y}} \quad , \end{aligned} \tag{3.16}$$

where the constant B is a weighted average of the vertical velocity over the plate:

$$B = \frac{1}{\pi}\int_0^1 \frac{u_z(y')}{\sqrt{y'(1-y')}}\mathrm{d}y'. \tag{3.17}$$

Thus we need to correct for the tangential velocity since it has a square root singularity at the edge of the plate. Apart from this, we can also calculate the vertical velocity outside the plate using (3.11)

$$u_z = \int_0^1 \frac{f(s)}{y-s}\mathrm{d}s, \quad y > 1 \quad .$$

Substituting (3.14) into the above equation and swapping the order of integration we get

$$u_z = \frac{1}{\pi^2}\int_0^1 u_z(y')\sqrt{\frac{1-y'}{y'}}\left(\int_0^1 \frac{1}{(y-s)(y'-s)}\sqrt{\frac{s}{1-s}}\mathrm{d}s\right)\mathrm{d}y' \quad .$$

Using contour integral techniques in App. C.1, we obtain the expression for the leading order behaviour as $y \to 1^+$

$$\begin{aligned} u_z &= \frac{1}{\pi^2}\int_0^1 u_z(y')\sqrt{\frac{1-y'}{y'}}\left(\pi\sqrt{\frac{y}{y-1}}\frac{1}{y'-y}\right)\mathrm{d}y' \\ \Rightarrow u_z\big|_{y\to 1^+} &\approx -\frac{1}{\pi\sqrt{y-1}}\int_0^1 u_z(y')\frac{1}{\sqrt{y'(1-y')}}\mathrm{d}y' \\ &= -\frac{B}{\sqrt{y-1}} \quad . \end{aligned} \tag{3.18}$$

We also see that the vertical velocity also has a square root singularity at the edge and this will also need to be corrected.

The pressure differential for the inviscid case can be calculated by using (3.4b), (3.5) and (3.15) to obtain the following expression:

$$[p] = 2\pi i\int_y^1 f(s)\mathrm{d}s \quad . \tag{3.19}$$

3.3.2 Correction to the Inviscid Solution

As seen in the previous section, both the tangential and vertical velocity need to be corrected. This means that we need to include viscosity into our governing equations for the fluid flow. Noting that we are solving a 2-D flow in the y and z coordinates, the component form of (3.3) is as follows:

$$-iu_y = -\frac{\partial p}{\partial y} + \frac{1}{\beta}\nabla^2 u_y \tag{3.20a}$$

$$-iu_z = -\frac{\partial p}{\partial z} + \frac{1}{\beta}\nabla^2 u_z \tag{3.20b}$$

$$\frac{\partial u_y}{\partial y} + \frac{\partial u_z}{\partial z} = 0 \tag{3.20c}$$

with

$$\nabla^2 = \frac{\partial^2}{\partial y^2} + \frac{\partial^2}{\partial z^2} \quad .$$

We introduce the stream function ψ

$$\begin{aligned} u_y &= -\frac{\partial \psi}{\partial z} \\ u_z &= \frac{\partial \psi}{\partial y} \end{aligned} \tag{3.21}$$

such that (3.20c) is automatically satisfied. Substituting (3.21) into (3.20a,b) and eliminating the pressure term by differentiating (3.20a) with respect to z and differentiating (3.20b) with respect to y and subtracting both equations, we obtain the following expression:

$$\nabla^2(\nabla^2 + i\beta)\psi = 0 \quad . \tag{3.22}$$

As we can see, excluding the second term inside the brackets is equivalent to the inviscid case where it satisfies Laplace's equation ($\nabla^2\phi = 0$) and therefore it is a first order approximation. In this correction, we propose a local coordinate system at the edge of the plate, given by

$$\begin{aligned} y &= 1 + \epsilon Y \\ z &= \epsilon Z \quad , \end{aligned} \tag{3.23}$$

where ϵ is some small but positive dimensionless number. In this new coordinate system, the origin is now at the edge of the plate and the plate is located in the negative X-axis (see Fig. 3.3).

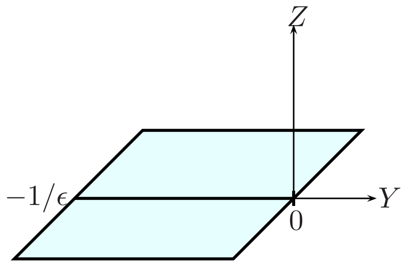

Figure 3.3: Coordinate system specified by (3.23) where the origin is at the edge of the plate. When $\beta \to \infty$, the clamped end of the plate ($Y = -1/\epsilon$) will tend to $-\infty$

Under the new coordinate system, we get the expression for the Laplacian operator (∇^2) to be

$$\nabla^2 = \frac{1}{\epsilon^2}\left(\frac{\partial^2}{\partial Y^2} + \frac{\partial^2}{\partial Z^2}\right) \quad .$$

We are interested in the case when β is large and so in order to make the two terms inside the bracket of (3.22) comparable in the new coordinate system, we require

$$\frac{1}{\epsilon^2} = \beta$$
$$\Rightarrow \epsilon = \frac{1}{\sqrt{\beta}}$$

We now take the Fourier transform of Y on (3.22) and we obtain the following differential equation in Z.

$$\frac{\partial^4\overline{\psi}}{\partial Z^4} + (i - 2\zeta^2)\frac{\partial^2\overline{\psi}}{\partial Z^2} + (\zeta^4 - i\zeta^2)\overline{\psi} = 0$$

The 4 independent solutions obtained from the differential equation are $e^{|\zeta|Z}$, $e^{-|\zeta|Z}$, $e^{\sqrt{\zeta^2-i}Z}$ and $e^{-\sqrt{\zeta^2-i}Z}$. We seek solutions that tend to zero at infinity since the fluid is not affected by the oscillations of the plate far away. Hence we construct the solution as

$$\overline{\psi} = \begin{cases} A_1(\zeta)e^{-\sqrt{\zeta^2-i}Z} - iB_1(\zeta)e^{-|\zeta|Z}, & Z > 0 \\ A_2(\zeta)e^{\sqrt{\zeta^2-i}Z} - iB_2(\zeta)e^{|\zeta|Z}, & Z < 0 \end{cases} \tag{3.24}$$

where $\sqrt{\zeta^2 - i}$ and $|\zeta|$ are defined to have positive real part and the functions A_1, A_2, B_1 and B_2 are to be determined from the boundary conditions. Using the expression for $\overline{\psi}$, the expressions for $\overline{u_y}$ and $\overline{u_z}$ can be easily obtained from the Fourier transform of Y of (3.21) and once those have been found, the pressure $\overline{p}$ as a function of Z can be obtained by taking the Fourier transform of (3.20b):

$$\overline{u_y} = \begin{cases} A_1(\zeta)\sqrt{\zeta^2-i}e^{-\sqrt{\zeta^2-i}Z} - iB_1(\zeta)|\zeta|e^{-|\zeta|Z}, & Z > 0 \\ -A_2(\zeta)\sqrt{\zeta^2-i}e^{\sqrt{\zeta^2-i}Z} + iB_2(\zeta)|\zeta|e^{|\zeta|Z}, & Z < 0 \end{cases} \tag{3.25a}$$

$$\overline{u_z} = \begin{cases} -i\zeta A_1(\zeta)e^{-\sqrt{\zeta^2-i}Z} - \zeta B_1(\zeta)e^{-|\zeta|Z}, & Z > 0 \\ -i\zeta A_2(\zeta)e^{\sqrt{\zeta^2-i}Z} - \zeta B_2(\zeta)e^{|\zeta|Z}, & Z < 0 \end{cases} \tag{3.25b}$$

$$\overline{p} = \begin{cases} i\epsilon\frac{|\zeta|}{\zeta}B_1(\zeta)e^{-|\zeta|Z}, & Z > 0 \\ -i\epsilon\frac{|\zeta|}{\zeta}B_2(\zeta)e^{|\zeta|Z}, & Z > 0 \end{cases} \tag{3.25c}$$

We now list down the boundary conditions at $Z = 0$ for the new solution.

- The velocity components are continuous across the plane $Z = 0$ with the tangential component equal to zero

$$
\begin{aligned}
u_y|_{Z=0^+} = u_y|_{Z=0^-} = 0 \\
u_z|_{Z=0^+} = u_z|_{Z=0^-}
\end{aligned}
\tag{3.26}
$$

- The tangential velocity outside the plate is zero and on the plate, it must cancel the velocity obtained from (3.16) and so

$$
u_y = \begin{cases} -\dfrac{B}{\sqrt{1-x}} = -\dfrac{B}{\sqrt{-\epsilon Y}}, & Y < 0 \\ 0, & Y > 0 \end{cases}
\tag{3.27}
$$

- The vertical velocity is zero on the plate, as it is already known and has been accounted for in the inviscid solution, and unknown outside the plate:

$$
u_z = \begin{cases} 0, & Y < 0 \\ \text{unknown function}, & Y > 0 \end{cases}
\tag{3.28}
$$

- The pressure differential on the plate is unknown and zero outside:

$$
[p] = \begin{cases} \text{unknown function}, & Y < 0 \\ 0, & Y > 0 \end{cases}
\tag{3.29}
$$

The first thing to notice from the boundary conditions is that $A_1(\zeta) = A_2(\zeta)$ and $B_1(\zeta) = B_2(\zeta)$. This comes directly from the boundary condition (3.26). Then the pressure differential from (3.25c) will have the expression

$$
\begin{aligned}
\overline{[p]} &= p|_{Z=0^+} - p|_{Z=0^-} \\
&= 2i\epsilon \frac{|\zeta|}{\zeta} B_1(\zeta) \quad .
\end{aligned}
\tag{3.30}
$$

Note that in Atkinson and de Lara's paper, the factor of ϵ is missing.

We will now use the Wiener-Hopf technique to find an expression for the pressure differential correction. We take the Fourier transform of the boundary conditions (3.27), (3.28) and (3.29). The half Fourier transform

$$\overline{F}_- = \int_{-\infty}^{0} F e^{i\zeta Y} \mathrm{d}Y$$

where the integral converges for $Im(\zeta) < 0$ and therefore $\overline{F}_-$ is a minus function since it is analytic in the lower half plane $Im(\zeta) < 0$ and denoted with a '-' subscript. Similiarly, the half Fourier transform

$$\overline{F}_+ = \int_{0}^{\infty} F e^{i\zeta Y} \mathrm{d}Y$$

where the integral converges for $Im(\zeta) > 0$ and therefore analytic in the upper half plane $Im(\zeta) > 0$. $\overline{F}_+$ is called a plus function and is indicated with a '+' subscript.

The Fourier transform of the boundary conditions simpifies to half Fourier transforms that are either analytic in the upper or lower half plane. Therefore, we can classify the velocity components and the pressure differential into plus and minus functions depending on where the region is non-zero. For the tangential velocity and the pressure differential, it is non-zero for $Y < 0$ and therefore $\overline{u_y}$ and $\overline{[p]}$ are minus functions and shall be denoted by $\overline{u_y} = \overline{u_y}_-$ and $\overline{[p]} = \overline{[p]}_-$ respectively. For the vertical velocity, it is non-zero for $Y > 0$ and therefore it is a plus function and shall be denoted as $\overline{u_z} = \overline{u_z}_+$.

So, for $Z = 0$, we have three equations which are (3.25a),(3.25b) and (3.30) involving 4 unknowns $\overline{[p]}_-$, $\overline{u_z}_+$, $A_1(\zeta)$ and $B_1(\zeta)$. Note that we have specified the boundary conditions for tangential velocity and so we know the form of $\overline{u_y}_-$. The explicit form of $\overline{u_y}$ will be considered as derived later for convenience. We can express $A_1(\zeta)$ and $B_1(\zeta)$ using (3.30) and (3.25a) to be in terms of $\overline{[p]}_-$ and $\overline{u_y}_-$.

$$\begin{aligned} A_1(\zeta) &= \frac{\zeta}{2\epsilon\sqrt{\zeta^2 - i}}\overline{[p]}_- + \frac{\overline{u_y}_-}{\sqrt{\zeta^2 - i}} \\ B_1(\zeta) &= \frac{\zeta}{2i\epsilon|\zeta|}\overline{[p]}_- \quad . \end{aligned}$$

Substituting into (3.25b) we obtain the following functional equation in terms of the two remaining unknowns $\overline{u_z}_+$ and $\overline{[p]}_-$

$$\begin{aligned} \overline{u_z}_+ &= \frac{i\zeta^2}{2\epsilon}\overline{[p]}_- \left[\frac{1}{|\zeta|} - \frac{1}{\sqrt{\zeta^2 - i}}\right] - \frac{i\zeta}{\sqrt{\zeta^2 - i}}\overline{u_y}_- \\ &= \frac{i\zeta^2}{2\epsilon|\zeta|\sqrt{\zeta^2 - i}}\overline{[p]}_-(\sqrt{\zeta^2 - i} - |\zeta|) - \frac{i\zeta}{\sqrt{\zeta^2 - i}}\overline{u_y}_- \\ &= \frac{i\zeta^2(\zeta^2 - i - |\zeta|^2)}{4\epsilon|\zeta|(\zeta^2 - i)}\left(\frac{2\sqrt{\zeta^2 - i}}{|\zeta| + \sqrt{\zeta^2 - i}}\right)\overline{[p]}_- - \frac{i\zeta}{\sqrt{\zeta^2 - i}}\overline{u_y}_- \end{aligned} \tag{3.31}$$

where in going from the second line to the third line, the first term on the RHS is multiplied by $2\sqrt{\zeta^2 - i}(|\zeta| + \sqrt{\zeta^2 - i})$ on the numerator and denominator. We see that this is of the form stated in the previous chapter in (2.1) with $\overline{u_y}_-$ known. We now define a function $H(\zeta)$ where

$$H(\zeta) = \frac{|\zeta| + \sqrt{\zeta^2 - i}}{2\sqrt{\zeta^2 - i}} \quad .$$

We see that $H(\zeta)$ is an even function and as $|\zeta| \to \infty$ that $H(\zeta) \to 1$ and it has no zeros on the real axis, thus containing the inversion contour for the inverse Fourier transform. This satisfies the condition to perform a product decomposition $H(\zeta) = H_+(\zeta)H_-(\zeta)$ as discussed in Sec. 2.3.

The function $|\zeta|$ is not an analytic function and thus we need another representation to make it analytic. Since (3.31) is defined on the real axis, we can represent $|\zeta|$ as

$$
\begin{aligned}
|\zeta| &= \lim_{\delta\to 0} \sqrt{\zeta + i\delta}\sqrt{\zeta - i\delta} \\
&= \sqrt{\zeta}_{+}\sqrt{\zeta}_{-} \qquad (3.32)
\end{aligned}
$$

since the branch point for $\sqrt{\zeta + i\delta}$ is in the lower half plane and $\sqrt{\zeta - i\delta}$ is in the upper half plane. Choosing both the branch cuts to be parallel to the real axis gives that $\sqrt{\zeta}_{+} = \lim_{\delta\to 0} \sqrt{\zeta + i\delta}$ is analytic in the upper half plane and therefore it is a plus function and similiarly $\sqrt{\zeta}_{-} = \lim_{\delta\to 0} \sqrt{\zeta - i\delta}$ is analytic in the lower half plane and therefore it is a minus function.

Thus, the function $H(\zeta)$ becomes

$$
H(\zeta) = \frac{\sqrt{\zeta}_{+}\sqrt{\zeta}_{-} + \sqrt{\zeta^2 - i}}{2\sqrt{\zeta^2 - i}} \quad .
$$

We shall refer to App. A on simplifying the expression for $H_{+}(\zeta)$ and $H_{-}(\zeta)$ and obtain their respective expansions as $|\zeta| \to \infty$.

Since (3.31) is defined only on the real axis, we note that in the first term on the RHS[1] of the equation that $(\zeta^2 - i - |\zeta|^2)$ is now equal to $-i$ since $|\zeta|^2 = \zeta^2$ here and so (3.31) now becomes

$$
\overline{u_z}_{+} = \frac{\zeta^2}{4\epsilon\sqrt{\zeta}_{+}\sqrt{\zeta}_{-}(\zeta - e^{i\pi/4})(\zeta + e^{i\pi/4})}\left(\frac{1}{H_{+}(\zeta)H_{-}(\zeta)}\right)\overline{[p]}_{-} - \frac{i\zeta}{\sqrt{\zeta^2 - i}}\overline{u_y}_{-}
$$

Rearranging the first term on the RHS so that the $\overline{[p]}_{-}$ term purely consists

[1]RHS=right hand side

of minus functions gives

$$\frac{\overline{u_z}_+(\zeta+e^{i\pi/4})H_+(\zeta)\sqrt{\zeta}_+}{\zeta}$$
$$=\frac{\zeta}{4\epsilon\sqrt{\zeta}_-(\zeta-e^{i\pi/4})H_-(\zeta)}\overline{[p]}_- - i\sqrt{\frac{\zeta+e^{i\pi/4}}{\zeta-e^{i\pi/4}}}H_+(\zeta)\sqrt{\zeta}_+\overline{u_y}_- \qquad (3.33)$$

We would not be able to proceed further until we know something about the form of $\overline{u_y}_-$. From the Fourier transform of (3.27), we get

$$\overline{u_y}_- = -e^{-i\pi/4}\frac{B}{\sqrt{\epsilon}}\frac{\sqrt{\pi}}{\sqrt{\zeta}_-} \quad .$$

Therefore (3.33) becomes

$$\frac{\overline{u_z}_+(\zeta+e^{i\pi/4})H_+(\zeta)\sqrt{\zeta}_+}{\zeta}$$
$$=\frac{\zeta}{4\epsilon\sqrt{\zeta}_-(\zeta-e^{i\pi/4})H_-(\zeta)}\overline{[p]}_- + \frac{B}{\sqrt{\epsilon}}\sqrt{\pi}e^{i\pi/4}\frac{\sqrt{\zeta}_+}{\sqrt{\zeta}_-}\sqrt{\frac{\zeta+e^{i\pi/4}}{\zeta-e^{i\pi/4}}}H_+(\zeta)$$
$$=\frac{\zeta}{4\epsilon\sqrt{\zeta}_-(\zeta-e^{i\pi/4})H_-(\zeta)}\overline{[p]}_- + \frac{B}{\sqrt{\epsilon}}\sqrt{\pi}e^{i\pi/4}\left[\frac{\sqrt{\zeta}_+}{\sqrt{\zeta}_-}\sqrt{\frac{\zeta+e^{i\pi/4}}{\zeta-e^{i\pi/4}}}-1\right]H_+(\zeta)$$
$$+\frac{B}{\sqrt{\epsilon}}\sqrt{\pi}e^{i\pi/4}H_+(\zeta) \quad .$$

We now define a function $S(\zeta)$ such that $S(\zeta)=S_+(\zeta)+S_-(\zeta)$ where

$$S(\zeta)=\left[\frac{\sqrt{\zeta}_+}{\sqrt{\zeta}_-}\sqrt{\frac{\zeta+e^{i\pi/4}}{\zeta-e^{i\pi/4}}}-1\right]H_+(\zeta) \quad .$$

Note that as $|\zeta|\to\infty$ we have that $S(\zeta)\to 0$ and therefore it satisfies the condition discussed in Sec.2.3. Thus we can perform a sum decomposition on $S(\zeta)$. We shall refer to App. B to simplify the expressions for $S_+(\zeta)$ and $S_-(\zeta)$ and to obtain their respective expansions as $|\zeta|\to\infty$. Once we have done the sum decomposition, we rearrange (3.33) so that all the plus functions are on one side of the equality and the minus functions are on the other side:

$$\frac{\overline{u_z}_+(\zeta+e^{i\pi/4})H_+(\zeta)\sqrt{\zeta_+}}{\zeta}-\frac{e^{i\pi/4}B\sqrt{\pi}}{\sqrt{\epsilon}}\left(S_+(\zeta)+H_+(\zeta)\right)$$
$$=\frac{\zeta}{4\epsilon\sqrt{\zeta_-}(\zeta-e^{i\pi/4})H_-(\zeta)}\overline{[p]}_-+\frac{e^{i\pi/4}B\sqrt{\pi}}{\sqrt{\epsilon}}S_-(\zeta)\equiv G(\zeta)\quad . \tag{3.34}$$

We have now re-expressed (3.31) into a function that consists of plus functions only on one side of the equality and a function that consists of minus functions only on the other side of the equality. On the LHS[2] of (3.34), the function is analytic in the lower half plane and the RHS of (3.34), the function is analytic in the upper half plane. Since we have that (3.34) holds on the real axis, by analytic continuation, we have that the function $G(\zeta)$ is analytic in the whole complex plane. The next step in the Wiener-Hopf method is to be able to use the generalised Liouville's theorem to be able to say what does the function $G(\zeta)$ is. In this case, we will be using the standard Liouville's theorem instead of the generalised version. To be able to do this we require some knowledge of the unknown functions $\overline{[p]}_-$ and $\overline{u_z}_+$.

The pressure differential at $Y=0$ can be singular but has to be integrable to give a finite force on the plate. More precisely, we expect a square root singularity in the pressure differential at the edge and therefore the Fourier transform of the pressure differential, $\overline{[p]}_-\sim 1/\sqrt{\zeta_-}$. At the same time, we also require that the vertical velocity outside the plate must correct the singular behaviour obtained in the inviscid solution. Therefore the Fourier transform of the vertical velocity outside the plate, $\overline{u_z}_+\sim 1/\sqrt{\zeta_+}$. Using these two facts together with the fact that the $H_+(\zeta), H_-(\zeta)\to 1$ and

[2]LHS=left hand side

$S_+(\zeta), S_-(\zeta) \to 0$ as $|\zeta| \to \infty$, we have shown that the LHS of (3.34) goes to a constant and the RHS of (3.34) goes to zero as $|\zeta| \to \infty$. By the standard Liouville's theorem, we have that the function $G(\zeta)$ is an entire function which is identically zero. We now have two equations with two unknowns, namely

$$\begin{aligned} \frac{\overline{u_z}_+(\zeta + e^{i\pi/4})H_+(\zeta)\sqrt{\zeta_+}}{\zeta} - \frac{e^{i\pi/4}B\sqrt{\pi}}{\sqrt{\epsilon}}\left(S_+(\zeta) + H_+(\zeta)\right) = 0 \quad , \\ \frac{\zeta}{4\epsilon\sqrt{\zeta_-}(\zeta - e^{i\pi/4})H_-(\zeta)}\overline{[p]}_- + \frac{e^{i\pi/4}B\sqrt{\pi}}{\sqrt{\epsilon}}S_-(\zeta) = 0 \quad . \end{aligned} \tag{3.35}$$

We are now able to solve for $\overline{[p]}_-$ and $\overline{u_z}_+$ using (3.35) to obtain the correction for the pressure differential. Since the correction is significant near the edge of the plate, we would use the expansion of the functions $H_+(\zeta)$, $H_-(\zeta)$, $S_+(\zeta)$ and $S_-(\zeta)$ as $|\zeta| \to \infty$ to get the leading order correction. Rearranging (3.35) and using binomial expansions, we get

$$\begin{aligned} \overline{u_z}_+|_{\zeta\to\infty} &\approx \frac{e^{i\pi/4}B\sqrt{\pi}}{\epsilon}\frac{1}{\sqrt{\zeta_+}} \quad , \\ \overline{[p]}_-|_{\zeta\to\infty} &\approx -\frac{2iB\epsilon\sqrt{2}\sqrt{\pi}}{\sqrt{\epsilon}}\frac{1}{\sqrt{\zeta_-}} \quad . \end{aligned} \tag{3.36}$$

Taking the inverse Fourier transform of the above equations and re-writing the equations in terms of the original variable y, we obtain

$$\begin{aligned} u_z|_{y\to1^+} &\approx \frac{B}{\sqrt{y-1}} \quad , \\ [p]|_{y\to1^-} &\approx 2\sqrt{2}e^{-i\pi/4}\epsilon B\frac{1}{\sqrt{1-y}} \quad . \end{aligned}$$

We see that the vertical velocity obtained from this correction cancels out the singularity obtained from the inviscid solution in (3.18) just outside the plate. As for the pressure differential, the correction has an added mass contribution out of phase with the velocity of the plate. This is clearly seen as the real part of the pressure differential. It also has a damping component which is in phase with the velocity of the plate which can be identified as the imaginary part of the term.

3.4 Equation of Motion of the Plate

Since we now have an expression for the force exerted by the fluid on the plate, mainly the pressure differential, we can now use it to solve the equation of motion for the vibrating plate. The force exerted by the fluid, f_{fluid}, is obtained by superposing the solution of the inviscid case and the correction to the invisicid case.

Atkinson and de Lara have made a simplification to calculating the pressure differential for the inviscid case. The correction to the inviscid case is mainly important near the edge at $y = 1$, the inviscid pressure differential is approximated by the pressure differential at the other end $y = 0$. Using (3.19) and setting $y = 0$, swapping order of integration and using contour integration techniques (App. C.2), we obtain the pressure differential at the clamped end to be

$$\begin{aligned}
[p] &= 2\pi i \int_0^1 f(s)\mathrm{d}s \\
&= 2\pi i \int_0^1 \int_0^1 \frac{1}{\pi^2}\sqrt{\frac{s}{1-s}}\frac{u_z(y')}{y'-s}\sqrt{\frac{1-y'}{y'}}\mathrm{d}s\mathrm{d}y' \\
&= 2\pi i \frac{1}{\pi^2}\int_0^1 (-\pi)u_z(y')\sqrt{\frac{1-y'}{y'}}\mathrm{d}y' \\
&= -2\pi^2 i \frac{1}{\pi^2}\int_0^1 u_z(y')\sqrt{\frac{1-y'}{y'}}\mathrm{d}y' \\
&= 2\pi^2 iA \quad ,
\end{aligned} \tag{3.37}$$

where A is given by (3.13). Therefore the full expression of the pressure differential by superposing the inviscid with the correction is

$$[p] = 2\pi^2 iA + 2\sqrt{2}e^{-i\pi/4}\epsilon B\frac{1}{\sqrt{1-y}} \quad . \tag{3.38}$$

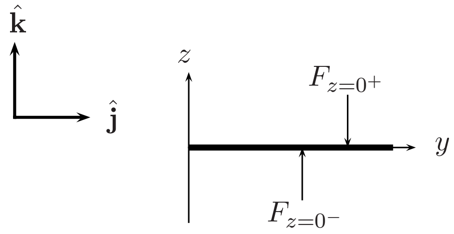

Figure 3.4: Forces acting on the plate

The fluid force can be calculated via the stress vector. The force per unit area exerted by the fluid on the top plate, $z = 0^+$, is $\mathbf{n} \cdot \mathbf{T}$ where $\mathbf{n}$ is the normal of the top plate, $\hat{\mathbf{k}}$, and $\mathbf{T}$ is the stress tensor (see Fig. 3.4). The force per unit area in the z-direction on the top plate is

$$\begin{aligned} F_{z=0^+} &= \mathbf{n} \cdot \mathbf{T} \cdot \hat{\mathbf{k}} \\ &= T_{zz} \\ &= -p|_{z=0^+} + \left.\frac{\partial u_z}{\partial z}\right|_{z=0^+} \quad . \end{aligned}$$

Using the continuity equation

$$\nabla \cdot \mathbf{u} = \frac{\partial u_y}{\partial y} + \frac{\partial u_z}{\partial z} = 0$$

and the no-slip condition on the surface of the plate, we find that the second term in the continuity equation vanishes since there is no horizontal velocity at the surface, thus giving the result

$$\left.\frac{\partial u_z}{\partial z}\right|_{z=0^+} = \left.\frac{\partial u_z}{\partial z}\right|_{z=0^-} = 0 \quad .$$

Therefore, the force on the top plate has been reduced to

$$F_{z=0^+} = -p|_{z=0^+} \quad .$$

Similiarly, the force on the bottom plate has the same form as the force on the top plate except for the minus sign. This comes from the fact that the normal of the bottom plate is $-\hat{\mathbf{k}}$. Putting all of these forces together, the net force of the fluid per unit area is the z-direction is

$$F_z = -p|_{z=0^+} + p|_{z=0^-} = -[p] \quad , \tag{3.39}$$

where this is the *dimensionless* force per unit area. We unscale back to the original pressure unit by multiplying the pressure differential by $\omega\rho LU$. Therefore, fluid force per unit area is

$$f_{\text{fluid}} = -\omega\rho LU\left(2\pi^2 iA + 2\sqrt{2}e^{-i\pi/4}\epsilon B\frac{1}{\sqrt{1-y}}\right) \quad .$$

Apart from the fluid force, we can also have a driving force for the plate as well. For simplicity, we model the driving force, f_{drive}, as a sinusoid with frequency ω and with strength equal to one on a line parallel to the clamping at a distance y_f away from the clamping and it is expressed in units of pressure

$$f_{\text{drive}} = \delta(y - y_f) \quad .$$

Note that this differs from Atkinson and de Lara by a factor of $e^{-i\omega t}$. This is because the driving force that they used is in the time domain and not the frequency domain as stated here. Both can be made equivalent by taking the Fourier transform of their driving force although they seem to have changed their definition for the Fourier transform to $e^{-i\omega t}$ instead of $e^{i\omega t}$ as used in solving the fluid force. This change of definition does not affect the rest of their analysis.

Using the expression for modelling a thin plate with a small deflection in the z-direction with an elastic restoring force while still assuming that all longitudinal cross sections act the same way [16], the equation of motioin of the plate can be reduced to

$$\rho_s h L \frac{\partial^2 w}{\partial t^2} + \frac{Eh^3}{12}\frac{\partial^4 w}{\partial y^4} = f^t_{\text{fluid}} + f^t_{\text{drive}} \quad , \tag{3.40}$$

where ρ_s is the density of the plate, w is the dimensionless deflection of the plate and h is the dimensionless thickness of the plate and E is the Young's modulus of the plate. w and h have both been scaled with respect to L. The forces are in the time domain as well. Taking the Fourier transform of (3.40), we get

$$\begin{aligned}
\frac{Eh^3}{12}\frac{\partial^4 w(y,\omega)}{\partial y^4} - \rho_s h L^2 \omega^2 w(y,\omega) &= \delta(y - y_f) - \omega\rho L U[p] \\
\frac{\partial^4 w(y,\omega)}{\partial y^4} - \frac{12}{Eh^2}\rho_s L^2 \omega^2 w(y,\omega) &= \frac{12}{Eh^3}\delta(y - y_f) - \frac{12}{Eh^3}\omega\rho L U[p] \\
\frac{\partial^4 w(y,\omega)}{\partial y^4} - c(\omega)^4 w(y,\omega) &= \frac{12}{Eh^3}\delta(y - y_f) - \frac{12}{Eh^3}\omega\rho L U[p] \quad ,
\end{aligned} \tag{3.41}$$

where $c(\omega)$ and $g(y,\omega)$ take the following expressions:

$$
\begin{aligned}
c(\omega) &= \left(\frac{3\rho_s}{E}\right)^{1/4} \left(\frac{2\omega L}{h}\right)^{1/2} \quad , \\
g(y,\omega) &= \frac{12}{Eh^3}\delta(y-y_f) - \frac{12}{Eh^3}\omega\rho LU[p] \quad .
\end{aligned}
$$

$[p]$ used here is the full expression for the pressure differential, given by (3.38). The boundary conditions for the plate are:

- Displacement is zero at $y = 0$

$$w|_{y=0} = 0 \quad .$$

- The first derivative is zero at $y = 0$ which represents clamping at the end

$$\frac{\partial w}{\partial y}|_{y=0} = 0 \quad .$$

- There is no bending moments at the free end $y = 1$ which can be written as

$$\frac{\partial^2 w}{\partial y^2}|_{y=1} = 0 \quad .$$

- There are no shearing forces at the free end $y = 1$ which can be written as

$$\frac{\partial^3 w}{\partial y^3}|_{y=1} = 0 \quad .$$

The constants A and B that appear in the RHS of (3.41) are weighted averages of the vertical velocity u_z. We can re-write this as the first derivative of w with respect to time. After scaling and taking the Fourier transform of the time variable, we find that

$$u_z(y) = -i\omega \frac{L}{U} w(y,\omega) \quad . \tag{3.42}$$

Atkinson and de Lara solved the equation of motion by constructing a solution to the equation of motion of the form

$$\begin{aligned} w(y,\omega) = w_p(y,\omega) &+ C_1 \sinh(c(\omega)y) + C_2 \cosh(c(\omega)y) + C_3 \sin(c(\omega)y) \\ &+ C_4 \cos(c(\omega)y) \quad , \end{aligned} \tag{3.43}$$

where $w_p(y,\omega)$ is constructed using the Green's function,$G(y',y')$, for equation (3.41)

$$w_p(y,\omega) = \int_0^1 G(y,y')g(y',\omega)\mathrm{d}y' \quad .$$

Their approach is very tedious since will we end up with an integral equation where the unknown $w(y,\omega)$ appears on both sides of the equation of (3.43) since $w_p(y,\omega)$ contains $w(y,\omega)$ in the constants A and B in $g(y,\omega)$. Hence, the method of Green's functions is not appropriate in this case.

Instead, we will use an eigenfunction expansion to solve the equation of motion. The homogeneous problem will be denoted as

$$\frac{\partial^4 \phi}{\partial y^4} - c_0^4 \phi = 0 \quad , \tag{3.44}$$

where c_0 is related to the resonant frequencies of the plate. The general solution to the homogenous problem is

$$\phi = C_1 \sinh(c_0 y) + C_2 \cosh(c_0 y) + C_3 \sin(c_0 y) + C_4 \cos(c_0 y) \quad .$$

Applying the boundary conditions to the solution of the homogeneous problem, we need to solve a homogenous linear system. Requiring that we must have non-trivial solutions, the determinant of the associated matrix of the linear system must be zero. We then find that there are certain values of c_0 can only be attained for non-trivial solutions and they satisfy the relation

$$1 + \cosh(c_{0,n}) \cos(c_{0,n}) = 0, \quad n \in \mathbb{N} \quad .$$

We can see that there are an infinite number of values of $c_{0,n}$ such that the above equation is satisfied. Using the boundary conditions, we can eliminate 3 of the coefficients of the general solution and the function ϕ can be written as an infinite sum

$$\begin{aligned} \phi = \sum_{n=1}^{\infty} C_n \Bigg[& \cosh(c_{0,n}y) - \cos(c_{0,n}y) \\ & + \frac{\cosh(c_{0,n}) + \cos(c_{0,n})}{\sinh(c_{0,n}) + \sin(c_{0,n})} \left(\sin(c_{0,n}y) - \sinh(c_{0,n}y)\right)\Bigg] \\ \Rightarrow \quad \phi = \sum_{n=1}^{\infty} & C_n \phi_n \quad , \end{aligned}$$

where ϕ_n are the basis functions for the solution and C_n are coefficients that depend on n. Each of the ϕ_n satisfies (3.44) and so we see that ϕ is a superposition of all the basis functions. Returning to solving (3.41), we expand the displacement in terms of the basis functions

$$w(y, \omega) = \sum_{n=1}^{\infty} w_m \phi_n(y, \omega) \tag{3.45}$$

and substitute it into (3.41) to get

$$\sum_{n=1}^{\infty} w_n \left(\phi_n^{(\mathrm{iv})}(y, \omega) - c(\omega)^4 \phi_n(y, \omega) \right) = g(y, \omega) \quad , \tag{3.46}$$

where

$$
\begin{aligned}
g(y,\omega) &= \frac{12}{Eh^3}\delta(y-y_f) - \frac{12}{Eh^3}\omega\rho LU\left(2\pi^2 iA + 2\sqrt{2}e^{-i\pi/4}\epsilon B\frac{1}{\sqrt{1-y}}\right) \\
&= \frac{12}{Eh^3}\delta(y-y_f) + \frac{24}{Eh^3}\rho\omega^2 L^2\left(\sum_{n=1}^{\infty} w_n\left[\int_0^1 \phi_n(y')\sqrt{\frac{1-y'}{y'}}\mathrm{d}y'\right.\right. \\
&\quad \left.\left.+\frac{\sqrt{2}}{\pi}e^{i\pi/4}\epsilon\frac{1}{\sqrt{1-y}}\int_0^1 \phi_n(y')\frac{1}{\sqrt{y'(1-y')}}\mathrm{d}y'\right]\right) \quad ,
\end{aligned}
$$

where we have used the expression for A and B from (3.13) and (3.17) and have substituted the relation between $u_z(y)$ with the displacement of the plate $w(y)$ from (3.42). We have the property of the basis functions that they are orthogonal to each other [8] and we can scale the basis functions so that

$$
\int_0^1 \phi_n(y)\phi_m(y)\mathrm{d}y = \begin{cases} 1, & \text{if } n = m \\ 0, & \text{if } n \neq m \end{cases}
$$

Multiplying $\phi_m(y,\omega)$ (3.46) and integrating from 0 to 1 and using the orthogonality relations above we get the following expression:

$$
\sum_{n=1}^{\infty} w_n\delta_{m,n}(c_{0,n}^4 - c^4)\int_0^1 \phi_m(y)\phi_n(y)\mathrm{d}y = \int_0^1 \phi_m(y)g(y)\mathrm{d}y \quad , \tag{3.47}
$$

where the RHS is

$$
\begin{aligned}
\int_0^1 \phi_m(y)g(y)\mathrm{d}y = &\frac{12}{Eh^3}\phi_m(y_f) + \frac{24}{Eh^3}\rho\omega^2 L^2 \times \\
&\left(\sum_{n=1}^{\infty} w_n\left[\int_0^1\int_0^1 \phi_m(y)\phi_n(y')\sqrt{\frac{1-y'}{y'}}\mathrm{d}y'\mathrm{d}y\right.\right. \\
&\left.\left.+\frac{\sqrt{2}}{\pi}e^{i\pi/4}\epsilon\int_0^1\int_0^1 \frac{1}{\sqrt{1-y}}\phi_m(y)\phi_n(y')\frac{1}{\sqrt{y'(1-y')}}\mathrm{d}y'\mathrm{d}y\right]\right) \quad .
\end{aligned}
$$

We will define the quantities

$$
\begin{aligned}
A_{m,n} &= \delta_{m,n}(c_{0,m}^4 - c^4)\int_0^1 \phi_m(y)\phi_n(y)\mathrm{d}y \\
B_{m,n} &= \int_0^1\int_0^1 \phi_m(y)\phi_n(y')\sqrt{\frac{1-y'}{y'}}\mathrm{d}y'\mathrm{d}y \\
C_{m,n} &= \int_0^1\int_0^1 \frac{1}{\sqrt{1-y}}\phi_m(y)\phi_n(y')\frac{1}{\sqrt{y'(1-y')}}\mathrm{d}y'\mathrm{d}y \quad .
\end{aligned}
$$

Therefore, (3.47) becomes

$$
\begin{aligned}
&\sum_{n=1}^{\infty} A_{m,n}w_m = \frac{12}{Eh^3}\phi_m(y_f) + \frac{24}{Eh^3}\rho\omega^2L^2\left(\sum_{n=1}^{\infty}\left[B_{m,n} + \frac{\sqrt{2}}{\pi}e^{i\pi/4}\epsilon C_{m,n}\right]w_n\right) \\
\Rightarrow \quad &\sum_{n=1}^{\infty}\left[A_{m,n} - \frac{24}{Eh^3}\rho\omega^2L^2\left(B_{m,n} + \frac{\sqrt{2}}{\pi}e^{i\pi/4}\epsilon C_{m,n}\right)\right]w_n = \frac{12}{Eh^3}\phi_m(y_f) \quad .
\end{aligned}
$$

This can now be written as a linear system

$$
D\mathbf{w} = \mathbf{r} \quad , \tag{3.48}
$$

where the matrix D has entries

$$
D_{m,n} = A_{m,n} - \frac{24}{Eh^3}\rho\omega^2L^2\left(B_{m,n} + \frac{\sqrt{2}}{\pi}e^{i\pi/4}\epsilon C_{m,n}\right)
$$

and the vector $\mathbf{r}$ has entries specified by

$$
r_m = \frac{12}{Eh^3}\phi_m(y_f) \quad .
$$

To solve this, we would have to truncate the series in (3.48) to include the first k terms and this will give a $k \times k$ matrix D where the entries will have to be computed numerically. Solving the linear system in (3.48) by using methods such as Gauss elimination (since in general the matrix

D is dense) gives the coefficients for the w_m. Thus we can calculate the displacement of the plate subjected to the driving force, the fluid force and the elastic restoring force of the plate from (3.45) for a given ω. We can also increase the accuracy of the solution by including more terms in the series and subsequently the matrix.

Chapter 4

Flexural and Torsional Vibrations

We would like to be able to test the method that was proposed by Atkinson and de Lara in using the Wiener-Hopf technique to obtain the leading order behaviour of a plate vibrating in a viscous fluid. Recently, Van Eysden and Sader [5] have solved the linearized Navier-Stokes equation exactly on a vibrating blade having normal and torsional oscillations for all values of Reynolds number. The solution comes from solving a system of linear equations where the entries of the matrix consist of Meijer-G functions. The authors have computed a quantity which is called the normalized hydrodynamic function, $\Gamma(\mathrm{Re})$, where Re is the Reynolds number for both cases. $\Gamma^n(\mathrm{Re})$ is for the case with normal oscillations and this is related to the force per unit *length*, f_{fluid}, exerted by the fluid on the blade while $\Gamma^t(\mathrm{Re})$ is for the case with torsional oscillations and it is related to the moment per unit *length*, m_{fluid} exerted by the fluid on the blade. Note that the forces that were calculated by Atkinson and de Lara [3] were in units of force per unit *area*. There is an extra term κ which signifies the wave number in the

z-direction but it can be shown that for $\kappa = 0$, the problem becomes a 2-D problem where it has infinite length in the x-direction. The general form of f_{fluid} and m_{fluid} for this geometry can be expressed as

$$f_{\text{fluid}} = \frac{\pi}{4}\rho\omega^2 L^2 \Gamma^n(\beta) w(x) \quad , \tag{4.1a}$$

$$m_{\text{fluid}} = -\frac{\pi}{8}\rho\omega^2 L^4 \Gamma^t(\beta) \Phi(x) \quad . \tag{4.1b}$$

To be consistent with the previous analysis, the Reynolds number will be denoted by β and note that it is the same definition used by the Atkinson and de Lara and L as the length across the blade. The functions $w(x)$ is the displacement of the blade as a function of x while $\Phi(x)$ is the angle of deflection of the blade as a function of x and is defined in both the papers by Van Eysden and Sader [5, 6]. This is because the displacement and the angle of the blade is the same for a specified value of x.

We will attempt to use the Wiener-Hopf method to capture the asymptotic behaviour of both cases for large values of β and will compare it with the tables that have been calculated from the exact solution.

4.1 Normal Oscillations in a Viscous Fluid

We will proceed with the same steps used in the previous chapter to calculate the inviscid solution and the correction to the inviscid solution and later obtain the force per unit length to be able to find out the hydrodynamic function $\Gamma^n(\beta)$. The superscript n in all the variables and constants here is to denote that it is for the normal oscillation case (see Fig. 4.1) and not raised to the power n.

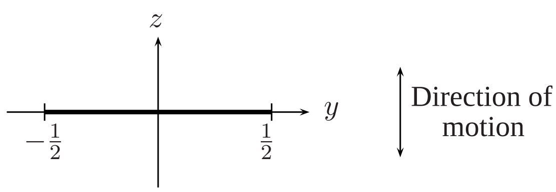

Figure 4.1: Blade performing normal oscillations

4.1.1 Inviscid Solution

In this problem, we have that the blade is centred at the origin and its edges are at $y = \pm 1/2$. The governing equation for the inviscid fluid is the same, namely Laplace's equation, where the velocity and the pressure can be determined by (3.4). The general solution for Laplace's equation for this case is superposing the fundamental solution with a function $f^n(s)$ which is to be determined from the boundary conditions over the length across the blade, which gives

$$\phi^n(y) = \int_{-1/2}^{1/2} f^n(s) \arctan\left(\frac{z}{y-s}\right) \mathrm{d}s \quad , \tag{4.2}$$

where $f^n(s)$ is to denote normal oscillations. The arctangent function still carries the same definition as in (3.7). We now list the boundary conditions on the plane $z = 0$ needed to specify the solution of Laplace's equation.

- The vertical velocity is continuous everywhere and known for the blade but unknown outside the blade. Also, we note that it is also symmetric about the origin:

$$u_z^n|_{z=0^+} = u_z^n|_{z=0^-} = \begin{cases} \text{unknown function}, & y > \left|\frac{1}{2}\right| \\ u_z(y), & y < \left|\frac{1}{2}\right| \end{cases} \tag{4.3}$$
$$u_z^n(y) = u_z^n(-y) \quad .$$

- The pressure differential is unknown for the blade but equal to zero outside the blade. Also, due to the symmetry of the problem, it is also symmetric about the origin:

$$[p]^n = \begin{cases} \text{unknown function to be determined,} & y < \left|\frac{1}{2}\right| \\ 0, & y > \left|\frac{1}{2}\right| \end{cases} \tag{4.4}$$
$$[p]^n(y) = [p]^n(-y) \quad .$$

We will also use the no-slip condition as a check for the inviscid solution as in the previous chapter. The vertical velocity is obtained by differentiating (4.2) with respect to z and setting $z = 0$ and using the boundary condition in (4.3), we obtain the following expression

$$u_z^n(y) = \int_{-1/2}^{1/2} \frac{f^n(s)}{y - s} \mathrm{d}s, \quad y < \left|\frac{1}{2}\right| \quad . \tag{4.5}$$

Using the same technique in the referred texts, the general solution for the function $f^n(s)$ is

$$\begin{aligned} f^n(s) &= \frac{1}{\pi^2\sqrt{1-4s^2}} \int_{-1/2}^{1/2} u_z^n(y') \frac{\sqrt{1-4y'^2}}{y'-s} \mathrm{d}y' + \frac{A}{\sqrt{1-4s^2}} \\ &= \frac{2s}{\pi^2\sqrt{1-4s^2}} \int_{0}^{1/2} u_z^n(y') \frac{\sqrt{1-4y'^2}}{y'^2-s^2} \mathrm{d}y' + \frac{A}{\sqrt{1-4s^2}} \quad , \end{aligned} \tag{4.6}$$

where in going from the first line to the second line we used the symmetry condition on the vertical velocity. At $z = 0^+$ and $z = 0^-$, (4.2) becomes

$$\begin{aligned} \phi^n_{z=0^+} &= \pi \int_y^{1/2} f^n(s)\mathrm{d}s \quad , \\ \phi^n_{z=0^-} &= -\pi \int_y^{1/2} f^n(s)\mathrm{d}s \quad . \end{aligned} \tag{4.7}$$

Therefore the pressure differential is

$$[p] = 2\pi i \int_{y}^{1/2} f^n(s)\mathrm{d}s \quad . \tag{4.8}$$

We now use the boundary condition (4.4) to set the constant A in (4.6). In other words, we require that $[p]^n = 0$ at $y = -1/2$

$$\begin{aligned}
&\Rightarrow \quad 0 = \int_{-1/2}^{1/2} f^n(s)\mathrm{d}s & (4.9)\\
&\Rightarrow \quad 0 = \int_{-1/2}^{1/2}\int_{0}^{1/2} u_z^n(y')\frac{2s}{\pi^2\sqrt{1-4s^2}}\frac{\sqrt{1-4y'^2}}{y'^2-s^2}\mathrm{d}y'\mathrm{d}s + \int_{-1/2}^{1/2}\frac{A}{\sqrt{1-4s^2}}\mathrm{d}s\\
&\Rightarrow \quad A = 0 \quad ,
\end{aligned}$$

since in the first term in the second line equals to zero because we are integrating over an odd function over a symmetric domain and thus $A = 0$. Therefore the function $f^n(s)$ is now

$$f^n(s) = \frac{2s}{\pi^2\sqrt{1-4s^2}}\int_{0}^{1/2} u_z^n(y')\frac{\sqrt{1-4y'^2}}{y'^2-s^2}\mathrm{d}y' \quad . \tag{4.10}$$

We now examine the behaviour of the tangential velocity of the inviscid solution. By taking the derivative with respect to y of (4.7), we have

$$u_y|_{z=0^+} = -\pi f^n(y) \quad . \tag{4.11}$$

As $y \to \pm 1/2$,

$$u_y^n|_{z=0^+} \approx \begin{cases} \dfrac{2\sqrt{2}}{\pi\sqrt{1-2y}} \displaystyle\int_0^{1/2} \dfrac{u_z^n(y')}{\sqrt{1-4y'^2}} \mathrm{d}y', & \text{as } y \to \left(\frac{1}{2}\right)_- \\ -\dfrac{2\sqrt{2}}{\pi\sqrt{1+2y}} \displaystyle\int_0^{1/2} \dfrac{u_z^n(y')}{\sqrt{1-4y'^2}} \mathrm{d}y', & \text{as } y \to \left(-\frac{1}{2}\right)_+ \end{cases}$$

$$= \begin{cases} \dfrac{B^n}{\sqrt{1-2y}}, & \text{as } y \to \left(\frac{1}{2}\right)^- \\ -\dfrac{B^n}{\sqrt{1+2y}}, & \text{as } y \to \left(-\frac{1}{2}\right)^+ \end{cases} , \tag{4.12}$$

where B^n is a weighted average of the vertical velocity,

$$B^n = \frac{2\sqrt{2}}{\pi} \int_0^{1/2} \frac{u_z^n(y')}{\sqrt{1-4y'^2}} \mathrm{d}y' \quad . \tag{4.13}$$

There is a singularity in the tangential velocity that needs to be corrected by including viscous effects. Also, we can use (4.5) to determine the vertical velocity outside the plate:

$$u_z^n(y) = \int_{-1/2}^{1/2} \frac{f^n(s)}{y-s} \mathrm{d}s, \quad y > \left|\frac{1}{2}\right| \quad .$$

Substituting (4.10) into the equation above and swapping the order of integration, we get

$$u_z^n(y) = \int_0^{1/2} \int_{-1/2}^{1/2} \frac{2s}{\pi^2\sqrt{1-4s^2}} u_z^n(y') \frac{\sqrt{1-4y'^2}}{y'^2 - s^2} \frac{1}{y-s} \mathrm{d}s\mathrm{d}y' \quad . \tag{4.14}$$

Using contour integration techniques (App. C.3), we obtain

$$
\begin{aligned}
u_z^n(y) &= \int_0^{1/2} \frac{2y}{\pi^2\sqrt{1-4y^2}} u_z^n(y') \frac{\sqrt{1-4y'^2}}{y'^2-y^2}(\pi i)\mathrm{d}y' \\
&\approx \begin{cases} -\dfrac{4i}{\pi\sqrt{2(1-2y)}} \displaystyle\int_0^{1/2} \frac{u_z^n(y')}{\sqrt{1-4y'^2}}\mathrm{d}y', & \text{as } y \to \left(\frac{1}{2}\right)^+ \\ \dfrac{4i}{\pi\sqrt{2(1+2y)}} \displaystyle\int_0^{1/2} \frac{u_z^n(y')}{\sqrt{1-4y'^2}}\mathrm{d}y', & \text{as } y \to \left(-\frac{1}{2}\right)^- \end{cases} \\
&= \begin{cases} -\dfrac{B^n}{\sqrt{2y-1}}, & \text{as } y \to \left(\frac{1}{2}\right)^+ \\ \dfrac{B^n i}{\sqrt{2y+1}}, & \text{as } y \to \left(-\frac{1}{2}\right)^- \end{cases} .
\end{aligned}
$$

We see that the vertical velocity also has a singular behaviour and needs to be corrected as well.

4.1.2 Correction to the Inviscid Solution

We will concentrate on retrieving the correction near the $y = 1/2$ edge. The analysis done in Sec.3.3.2 is the same here except instead of using the change of variables stated in (3.23), we will use

$$
\begin{aligned}
y &= \frac{1}{2} + \epsilon Y \\
z &= \epsilon Z \quad ,
\end{aligned}
\tag{4.15}
$$

where $\epsilon = 1/\sqrt{\beta}$ as usual. The governing equation (3.22) is the same in this case and so taking the Fourier transform of this equation and solving it, gives the same expression for $\overline{\psi}^n$ in (3.24) and therefore the expressions for $\overline{u_y}^n$, $\overline{u_z}^n$ and $\overline{[p]}^n$ are the same as in (3.25). The boundary conditions (3.26), (3.28) and (3.29) are all the same except for the condition on the tangential velocity in (3.27).

The tangential velocity on the blade must cancel the singular behaviour obtained in the inviscid solution in (4.12) and it is zero outside the plate. Therefore, we have

$$u_y^n = \begin{cases} -\dfrac{B^n}{\sqrt{1-2y}} = -\dfrac{B^n}{\sqrt{2}}\dfrac{1}{\sqrt{-\epsilon Y}} = -\dfrac{B'^n}{\sqrt{-\epsilon Y}}, & Y < 0 \\ 0, & Y > 0 \end{cases}$$

where we have used (4.15) and $B'^n = B^n/\sqrt{2}$. Notice that the analysis from here onwards is the same as in Sec.3.3.2 except we just replace B with B'^n. Hence we can immediately write down the expressions for $\overline{u_z}^n$ and $\overline{[p]}^n$ as $|\zeta| \to \infty$ using (3.36)

$$\begin{aligned} \overline{u_z}^n_+|_{|\zeta|\to\infty} &\approx \frac{e^{i\pi/4}B'^n\sqrt{\pi}}{\epsilon}\frac{1}{\sqrt{\zeta_+}} \\ \overline{[p]}^n_-|_{|\zeta|\to\infty} &\approx -\frac{2iB'^n\epsilon\sqrt{2}\sqrt{\pi}}{\sqrt{\epsilon}}\frac{1}{\sqrt{\zeta_-}} \end{aligned}$$

Taking the inverse Fourier transform and re-writing it in the original variables y, we get

$$u_z^n \approx \frac{B'^n}{\sqrt{\epsilon Y}} = \frac{B^n}{\sqrt{2\epsilon Y}} = \frac{B^n}{\sqrt{2y-1}} \tag{4.16a}$$

$$[p]^n \approx \frac{2\sqrt{2}B'^n\epsilon e^{-i\pi/4}}{\sqrt{-\epsilon Y}} = \frac{2\sqrt{2}B^n\epsilon e^{-i\pi/4}}{\sqrt{-2\epsilon Y}} = \frac{2\sqrt{2}B^n\epsilon e^{-i\pi/4}}{\sqrt{1-2y}} \tag{4.16b}$$

We have now obtained the correction for the pressure differential at the edge $y = 1/2$. We can repeat a rather similiar analysis for the edge $y = -1/2$, performing the same steps as described in Sec. 3.3.2. However, a simple argument will help shorten the computation to obtain the pressure differential at the edge $y = -1/2$. For the blade that performs normal oscillations, the pressure is symmetric about the origin. Therefore the correction to the pressure differential near $y = -1/2$ would have the same form as (4.16b) except with the with the term $\sqrt{1-2y}$ replaced with $\sqrt{1+2y}$. The total correction for the pressure differential, $[p]_c^n$, is just summing the contributions from each end of the blade giving

$$[p]_c^n = 2\sqrt{2}B^n \epsilon e^{-i\pi/4} \left(\frac{1}{\sqrt{1-2y}} + \frac{1}{\sqrt{1+2y}} \right) \quad .$$

From the above equation, it is clear that it is symmetric in the region $-1/2 < y < 1/2$. When repeating the analysis for the edge $y = -1/2$, it can be shown that the vertical velocity cancels the singular behaviour outside the blade as well.

4.1.3 Hydrodynamic Function $\Gamma^n(\beta)$

We proceed to calculate the force per unit length exerted by the fluid on the blade. The pressure differential is the sum of the inviscid contribution and the total correction of the inviscid case

$$[p]^n = 2\pi i \int_y^{1/2} f^n(s)\mathrm{d}s + 2\sqrt{2}B^n \epsilon e^{-i\pi/4} \left(\frac{1}{\sqrt{1-2y}} + \frac{1}{\sqrt{1+2y}} \right) \quad . \tag{4.17}$$

As in the previous chapter in (3.39), we have found that the net force excerted by the fluid on the blade in the z-direction is

$$F_z = -[p]^n \quad .$$

This gives the dimensionless force per unit area. To obtain the force per unit length, we have to integrate the above expression over the length of the blade and multiplying by $\omega\rho LU$ and thus

$$f_{\text{fluid}} = -\omega\rho LU \int_{-1/2}^{1/2} [p]^n \mathrm{d}y \quad . \tag{4.18}$$

Substituting (4.17) into (4.18), and swapping order of integration we get,

$$
\begin{aligned}
f_{\text{fluid}} &= -\omega\rho LU \left[2\pi i \int_{-1/2}^{1/2} \int_{-1/2}^{y} f^n(s) \mathrm{d}y \mathrm{d}s \right. \\
&\qquad \left. + 2\sqrt{2} B^n \epsilon e^{-i\pi/4} \int_{-1/2}^{1/2} \left(\frac{1}{\sqrt{1-2y}} + \frac{1}{\sqrt{1+2y}} \right) \mathrm{d}y \right] \\
&= -\omega\rho LU \left[2\pi i \int_{-1/2}^{1/2} (s+1/2) f^n(s) \mathrm{d}s + 2\sqrt{2} B^n \epsilon e^{-i\pi/4} (2\sqrt{2}) \right] \\
&= -\omega\rho LU \left[2\pi i \int_{-1/2}^{1/2} s f(s) \mathrm{d}s + 8 B^n \epsilon e^{-i\pi/4} \right] \qquad (4.19)
\end{aligned}
$$

since $\int_{-1/2}^{1/2} f^n(s)\mathrm{d}s = 0$ from (4.9). Substituting $f^n(s)$ from (4.10) into the first term and swapping the order of integration, the integral can be reduced using contour integration techniques (App. C.4) to give

$$
\begin{aligned}
f_{\text{fluid}} = -\omega\rho LU &\left[2\pi i \int_{0}^{1/2} \left(-\frac{\pi}{2} \right) \frac{2}{\pi^2} u_z^n(y') \sqrt{1-4y'^2} \mathrm{d}y' \right. \\
&\left. + \frac{16\sqrt{2}}{\pi} \epsilon e^{-i\pi/4} \int_{0}^{1/2} \frac{u_z^n(y')}{\sqrt{1-4y'^2}} \mathrm{d}y' \right] \quad , \qquad (4.20)
\end{aligned}
$$

where we have used the expression for B^n from (4.13). We can re-write the vertical velocity in terms of the first derivative of the displacement of the blade with respect to time, t, noting that the displacement is a function of x and not y. Therefore, after taking the Fourier transform of the time derivative and scaling, we get

$$
u_z^n(y) = -i\omega \frac{L}{U} w(x) \quad .
$$

Substituting $u_z^n(y)$ into (4.20), re-arranging the terms and performing the integrals which are elementary, we obtain

$$f_{\text{fluid}} = \frac{\pi}{4}\rho\omega^2 L^2 \left[1 + \frac{16\sqrt{2}}{\pi}\epsilon e^{i\pi/4}\right] w(x) \quad .$$

We can now identify that the hydrodynamic function from (4.1a) for the case of normal oscillations is

$$\Gamma^n(\beta) = 1 + \frac{16\sqrt{2}}{\pi\sqrt{\beta}} e^{i\pi/4} \quad . \tag{4.21}$$

4.2 Torsional Oscillations in a Viscous Fluid

We shift our attention to use the method on to a blade which undergoes torsional oscillations (see Fig. 4.2). The inviscid solution is first obtained and subsequently the correction to the inviscid solution. These are to be used later to compute the moment per unit length to determine the form of the hydrodynamic function $\Gamma^t(\beta)$. The superscript t in all the variables and constants here is to denote case of the torsional oscillation and not raised to the power t.

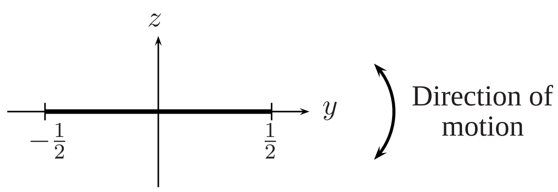

Figure 4.2: Blade performing torsional oscillations

4.2.1 Inviscid Solution

As for the normal oscillation case, the governing equation for the inviscid fluid is Laplace's equation and as usual, the velocity and pressure profile can be determined using (3.4). The potential ϕ^t is still of the form in (4.2) where $f^t(s)$ is denoted for torsional oscillations is to be determined by the boundary conditions.

The boundary conditions are the same as in (4.3) and (4.4) except that instead of having the vertical velocity and the pressure differential to be symmetric, we require that they are antisymmetric:

$$\begin{aligned} u_z^t(y) &= -u_z^t(-y) \quad , \\ [p]^t(y) &= -[p]^t(-y) \quad . \end{aligned} \tag{4.22}$$

The general form of the function $f^t(s)$ is the same as in the previous case, that is

$$f^t(s) = \frac{1}{\pi^2\sqrt{1-4s^2}} \int_{-1/2}^{1/2} u_z^t(y') \frac{\sqrt{1-4y'^2}}{y'-s} \mathrm{d}y' + \frac{A}{\sqrt{1-4s^2}} \quad .$$

Using the antisymmetric condition for the vertical velocity in (4.22),

$$f^t(s) = \frac{2}{\pi^2\sqrt{1-4s^2}} \int_{0}^{1/2} u_z^t(y') \frac{y'\sqrt{1-4y'^2}}{y'^2-s^2} \mathrm{d}y' + \frac{A}{\sqrt{1-4s^2}} \quad . \tag{4.23}$$

The pressure differential is still has the same form as in (4.8). Using the boundary condition in (4.4) that the pressure differential is zero at $y = -1/2$, we have that

$$\int_{-1/2}^{1/2} f^t(s) \mathrm{d}s = 0 \quad . \tag{4.24}$$

Substituting $f^t(s)$ from (4.23) into the above equation and swapping order of integration,

$$\int_0^{1/2}\int_{-1/2}^{1/2} \frac{2}{\pi^2\sqrt{1-4s^2}} u_z^t(y') \frac{y'\sqrt{1-4y'^2}}{y'^2-s^2} \mathrm{d}s\mathrm{d}y' + \int_{-1/2}^{1/2} \frac{A}{\sqrt{1-4s^2}} \mathrm{d}s = 0 \quad . \tag{4.25}$$

Using contour integration techniques (App. C.5) on the first term, we find that the term vanishes and thus we find that $A = 0$. The function $f(s)$ is now

$$f^t(s) = \frac{2}{\pi^2\sqrt{1-4s^2}} \int_0^{1/2} u_z^t(y') \frac{y'\sqrt{1-4y'^2}}{y'^2 - s^2} \mathrm{d}y' \quad . \tag{4.26}$$

Using the the expression for the tangential velocity from (4.11) for $z = 0^+$,

$$\begin{aligned}
u_y^t|_{z=0^+} &= -\frac{2\pi}{\pi^2\sqrt{1-4y^2}} \int_0^{1/2} u_z^t(y') \frac{y'\sqrt{1-4y'^2}}{y'^2 - y^2} \mathrm{d}y' \\
&\approx \frac{8}{\pi\sqrt{1-4y^2}} \int_0^{1/2} u_z^t(y') \frac{y'}{\sqrt{1-4y'^2}} \mathrm{d}y' \\
&= \begin{cases} \dfrac{4\sqrt{2}}{\pi\sqrt{1-2y}} \displaystyle\int_0^{1/2} u_z^t(y') \frac{y'}{\sqrt{1-4y'^2}} \mathrm{d}y', & y \to \left(\frac{1}{2}\right)^- \\ \dfrac{4\sqrt{2}}{\pi\sqrt{1+2y}} \displaystyle\int_0^{1/2} u_z^t(y') \frac{y'}{\sqrt{1-4y'^2}} \mathrm{d}y', & y \to \left(-\frac{1}{2}\right)^+ \end{cases} \\
&= \begin{cases} \dfrac{B^t}{\sqrt{1-2y}}, & y \to \left(\frac{1}{2}\right)^- \\ \dfrac{B^t}{\sqrt{1+2y}}, & y \to \left(-\frac{1}{2}\right)^+ \end{cases} \quad ,
\end{aligned} \tag{4.27}$$

where B^t is a weighted average of the vertical velocity

$$B^t = \frac{4\sqrt{2}}{\pi} \int_0^{1/2} u_z^t(y') \frac{y'}{\sqrt{1-4y'^2}} \mathrm{d}y' \quad . \tag{4.28}$$

We see that there is a singular behaviour near the edges of the plate and this will have to be corrected

Using the expresion in (4.5) to determine the vertical velocity outside the blade,

$$u_z^t(y) = \int_{-1/2}^{1/2} \frac{f^t(s)}{y - s} \mathrm{d}s, \quad y > \left|\frac{1}{2}\right| \quad .$$

Substituting (4.26) into the above equation and swapping order of integration gives

$$u_z^t(y) = \int_0^{1/2} \int_{-1/2}^{1/2} \frac{2}{\pi^2\sqrt{1-4s^2}} \frac{u_z^t(y')}{y-s} \frac{y'\sqrt{1-4y'^2}}{y'^2-s^2} \mathrm{d}s\mathrm{d}y' \quad . \tag{4.29}$$

Using contour integration techniques (App. C.6), the vertical velocity will now have the form

$$\begin{aligned}
u_z^t(y) &= \int_0^{1/2} (\pi i) u_z^t(y') \frac{2y'}{\pi^2\sqrt{1-4y^2}} \frac{\sqrt{1-4y'^2}}{y'^2-y^2} \mathrm{d}y' \\
&\approx -\frac{8i}{\pi\sqrt{1-4y^2}} \int_0^{1/2} u_z^t(y') \frac{y'}{\sqrt{1-4y'^2}} \mathrm{d}y' \\
&= \begin{cases} -\dfrac{4\sqrt{2}}{\pi\sqrt{2y-1}} \displaystyle\int_0^{1/2} u_z^t(y') \frac{y'}{\sqrt{1-4y'^2}} \mathrm{d}y', & y \to \left(\frac{1}{2}\right)^- \\ -\dfrac{4i\sqrt{2}}{\pi\sqrt{2y+1}} \displaystyle\int_0^{1/2} u_z^t(y') \frac{y'}{\sqrt{1-4y'^2}} \mathrm{d}y', & y \to \left(-\frac{1}{2}\right)^+ \end{cases} \\
&= \begin{cases} -\dfrac{B^t}{\sqrt{2y-1}}, & y \to \left(\frac{1}{2}\right)^- \\ -\dfrac{B^t i}{\sqrt{2y+1}}, & y \to \left(-\frac{1}{2}\right)^+ \end{cases} \quad .
\end{aligned}$$

The vertical velocity outside the plate needs to be corrected for the singular behaviour outside the plate.

4.2.2 Correction to the Inviscid Solution

As with the previous section, we shall start by looking at the edge $y = 1/2$. The change of variables to a local coordinate system at the edge is the same in the previous section in (4.15). The governing equation is still the same as in the previous chapter and we have the same expressions for $\overline{u_y}^t$, $\overline{u_z}^t$ and $\overline{[p]}^t$ in (3.25). As usual, the boundary conditions are the same except for the tangential velocity.

The tangential velocity on the blade has to cancel the singular behaviour obtained in the inviscid solution in (4.27) and outside the blade it is zero.

Thus, the boundary condition for the tangential velocity is given as

$$\overline{u_y}^t = \begin{cases} -\dfrac{B^t}{\sqrt{1-2y}} = -\dfrac{B^t}{\sqrt{-2\epsilon Y}} = -\dfrac{B'^t}{\sqrt{-\epsilon Y}}, & Y < 0 \\ 0, & Y > 0 \end{cases} \quad ,$$

where we have used the local coordinate system in the previous section and $B'^t = B^t/\sqrt{2}$ where B is defined in (4.28)

We have again that this is the same case as before in Sec. 3.3.2 except with B replaced by B'^t. Thus we can straight away write down the expression for the vertical velocity and pressure differential in terms of the original variable y but with the definition of B^t in (4.28).

$$u_z^t \approx \frac{B'^t}{\sqrt{\epsilon Y}} = \frac{B^t}{\sqrt{2\epsilon Y}} = \frac{B^t}{\sqrt{2y-1}} \tag{4.30a}$$

$$[p]^t \approx \frac{2\sqrt{2}B'^t\epsilon e^{-i\pi/4}}{\sqrt{-\epsilon Y}} = \frac{2\sqrt{2}B^t\epsilon e^{-i\pi/4}}{\sqrt{-2\epsilon Y}} = \frac{2\sqrt{2}B^t\epsilon e^{-i\pi/4}}{\sqrt{1-2y}} \quad . \tag{4.30b}$$

As usual, the singular behaviour for the vertical velocity has been canceled and have a square root singularity for the pressure differential.

We can repeat the procedure for the edge $y = -1/2$ but we shall use a similiar argument in the previous section to obtain the correction. Noting that, just as the vertical velocity is antisymmetric about the origin, so too the pressure differential is antisymmetric about the origin as well. Therefore, the correction to the pressure differential at the edge $y = -1/2$ is the same as in (4.30b) except that it has a minus sign and the term $\sqrt{1-2y}$ is replaced with $\sqrt{1+2y}$. Hence, the total correction to the pressure differential, $[p]_c^t$, is

$$[p]_c^t = 2\sqrt{2}B\epsilon e^{-i\pi/4}\left(\frac{1}{\sqrt{1-2y}} - \frac{1}{\sqrt{1+2y}}\right) \quad .$$

4.2.3 Hydrodynamic Function $\Gamma^t(\beta)$

The total pressure differential is the sum of the inviscid part and the correction

$$[p]^t = 2\pi i \int_y^{1/2} f^t(s)\mathrm{d}s + 2\sqrt{2}B^t \epsilon e^{-i\pi/4}\left(\frac{1}{\sqrt{1-2y}} - \frac{1}{\sqrt{1+2y}}\right) \quad . \quad (4.31)$$

It not appropriate to consider the force per unit length on a blade performing torsional oscillations since the pressure differential is antisymmetric and so the total force per unit length on the blade is zero. Instead, we calculate the moment per unit length of the blade.

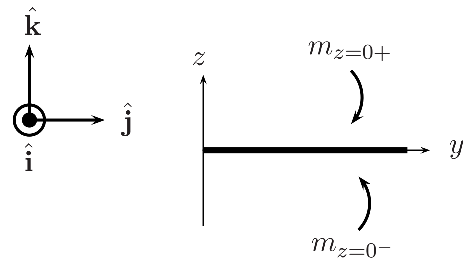

Figure 4.3: Moments experienced by the blade. The $\hat{\mathbf{i}}$-direction is pointing out of the page

The moment caused by the force acting on the top plate about the origin is force on the top plate multiplied by the perpendicular distance from the origin:

$$m_{z=0^+} = -yF_{z=0^+}$$

since in a right-handed coordinate system, the moment is positive if it is acting to rotate in the anti-clockwise direction. The moment caused by the force on the top blade is acting to rotate in the clockwise direction, hence the minus sign (see Fig. 4.3). Similiarly, the moment caused by the force on the bottom blade about the origin is

$$m_{z=0^-} = yF_{z=0^-} \quad .$$

So, the *dimensionless* net moment per unit area experienced by the blade about the origin is

$$m_{\text{net}} = -yF_z \quad .$$

The moment per unit length can be found by integrating the net moment across the length of the blade

$$\begin{aligned} m_{\text{fluid}} &= -L \int_{-1/2}^{1/2} yF_z \mathrm{d}y \\ &= \omega\rho L^2 U \int_{-1/2}^{1/2} y[p]^t \mathrm{d}y \quad , \end{aligned}$$

where F_z is the net force in the z-direction. Substituting (4.31) into the above equation and swapping the order of integration,

$$\begin{aligned} m_{\text{fluid}} = \omega\rho L^2 U & \left[2\pi i \int_{-1/2}^{1/2} \int_{-1/2}^{s} y f^t(s) \mathrm{d}y \mathrm{d}s \right. \\ & \left. + 2\sqrt{2} B^t \epsilon e^{-i\pi/4} \int_{-1/2}^{1/2} \frac{y}{\sqrt{1-2y}} - \frac{y}{\sqrt{1+2y}} \mathrm{d}y \right] \\ = \omega\rho L^2 U & \left[\pi i \int_{-1/2}^{1/2} (s^2 - \frac{1}{4}) f^t(s) \mathrm{d}s + 2\sqrt{2} B \epsilon e^{-i\pi/4} \left(\frac{2}{\sqrt{3}} \right) \right] \\ = \omega\rho L^2 U & \left[\pi i \int_{-1/2}^{1/2} s^2 f^t(s) \mathrm{d}s + 2\sqrt{2} B^t \epsilon e^{-i\pi/4} \left(\frac{2}{\sqrt{3}} \right) \right] \end{aligned}$$

since $\int_{-1/2}^{1/2} f^t(s)\mathrm{d}s = 0$ from (4.24). Substituting the expression for $f^t(s)$ from (4.26) and B^t from (4.28), swapping the order of integration and performing contour integration (App. C.4)

$$
\begin{aligned}
m_{\text{fluid}} = \omega\rho L^2 U \Bigg[& \pi i \int_0^{1/2} \int_{-1/2}^{1/2} \frac{2s^2}{\pi^2\sqrt{1-4s^2}} \frac{y'\sqrt{1-4y'^2}}{y'^2 - s^2} u_z^t(y') \mathrm{d}s\mathrm{d}y' \\
& + \frac{16\sqrt{2}}{3\pi} \epsilon e^{-i\pi/4} \int_0^{1/2} \frac{y'}{\sqrt{1-4y'^2}} u_z^t(y') \mathrm{d}y' \Bigg] \\
= \omega\rho L^2 U \Bigg[& \pi i \int_0^{1/2} \left(-\frac{\pi}{2}\right) \frac{2y'\sqrt{1-4y'^2}}{\pi^2} u_z^t(y') \mathrm{d}y' \\
& + \frac{16\sqrt{2}}{3\pi} \epsilon e^{-i\pi/4} \int_0^{1/2} \frac{y'}{\sqrt{1-4y'^2}} u_z^t(y') \mathrm{d}y' \Bigg] \\
= \omega\rho L^2 U \Bigg[& -i \int_0^{1/2} y' u_z^t(y') \sqrt{1-4y'^2} \mathrm{d}y' \\
& + \frac{16\sqrt{2}}{3\pi} \epsilon e^{-i\pi/4} \int_0^{1/2} \frac{y'}{\sqrt{1-4y'^2}} u_z^t(y') \mathrm{d}y' \Bigg] \quad . \qquad (4.32)
\end{aligned}
$$

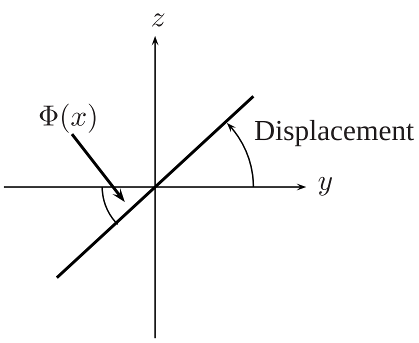

Figure 4.4: Displacement and the function $\Phi(x)$ for torsional oscillations

We can replace the vertical velocity as the first derivative with respect to time of the displacement of the blade. Because it is executing torsional oscillations, the displacement is defined by the arc traced by the edges with respect to the $z = 0$ plane (see Fig. 4.4). Taking the Fourier transform of the first derivative with respect to time and unscaling,

$$u_z^t(y) = -i\omega \frac{L^2}{U} y\Phi(x) \quad ,$$

where $\Phi(x)$[1] is the angle of the blade with respect to $z = 0$. Substituting the vertical velocity into (4.32) and performing the integrals which again are elementary,

$$
\begin{aligned}
m_{\text{fluid}} &= -\rho\omega^2 L^4 \left[\int_0^{1/2} y'^2 \sqrt{1-4y'^2}\mathrm{d}y' + \frac{16\sqrt{2}}{3\pi}\epsilon e^{i\pi/4}\int_0^{1/2} \frac{y'^2}{\sqrt{1-4y'^2}}\mathrm{d}y'\right]\Phi(x) \\
&= -\rho\omega^2 L^4 \left[\frac{\pi}{128} + \frac{16\sqrt{2}}{3\pi}\epsilon e^{i\pi/4}\frac{\pi}{32}\right]\Phi(x) \\
&= -\frac{\pi}{8}\rho\omega^2 L^4 \left[\frac{1}{16} + \frac{4\sqrt{2}}{3\pi}\epsilon e^{i\pi/4}\right]\Phi(x) \quad .
\end{aligned}
$$

We can immediately identify from (4.1b) that the hydrodynamic function for the case of a blade having torsional oscillations is given by

$$
\Gamma^n(\beta) = \frac{1}{16} + \frac{4\sqrt{2}}{3\pi\sqrt{\beta}}e^{i\pi/4} \quad . \tag{4.33}
$$

[1] $\Phi(x)$ has units $1/L$ as defined in [5]

Chapter 5

Results and Discussion

5.1 Comparison with Exact Computed results

Having found the hydrodynamic function for both the cases of normal and torsional oscillation, we are now able to compare results with the exact solution that was found by Van Eysden and Sader [6]. The hydrodynamic function consists of a real and imaginary component that depends on the Reynolds number, β. The real component is the inertial component of the force exerted by the fluid. This can be thought of as the force needed to move a mass of fluid as the blade oscillates. The imaginary component is the dissipative component of the force which acts to dampen the oscillation of the blade or the drag force. Thus we will compare the numerics of the inertial and the dissipative force for a range of values for β.

Since the method that was used to calculate the hydrodynamic function in this thesis is based on the assumption that the Reynolds number is large, we shall compare the results for $\log_{10}\beta > 1$. Note that the results that are relevant to this thesis for comparison of the exact numerics from Van Eysden and Sader's paper is the $\kappa = 0$ column. Using the formulas for the hydrodynamic function $\Gamma^n(\beta)$ and $\Gamma^t(\beta)$ from (4.21) and (4.33), we can calculate the real and imaginary parts of the functions for various β and the results are as below

	Normal		Torsional	
$\log_{10}\beta$	$\mathrm{Re}(\Gamma^n(\beta))$	$\mathrm{Im}(\Gamma^n(\beta))$	$\mathrm{Re}(\Gamma^t(\beta))$	$\mathrm{Im}(\Gamma^t(\beta))$
1.0	2.61053	1.61053	0.196711	0.134211
1.5	1.90567	0.90567	0.137973	0.0754725
2.0	1.5093	0.509296	0.104941	0.0424413
2.5	1.2864	0.286398	0.0863665	0.0238665
3.0	1.16105	0.161053	0.0759211	0.0134211
3.5	1.09057	0.090567	0.0700473	0.00754725
4.0	1.05093	0.0509296	0.0667441	0.00424413
∞	1	-	0.0625	-

Table 5.1: Computed real and imaginary components of the hydrodynamic function $\Gamma^n(\beta)$ and $\Gamma^t(\beta)$ for normal and torsional oscillations respectively as a function of β using the Wiener-Hopf method

As we can see from Table 5.1, the result from using the Wiener-Hopf method follows the same trend but does not give the right numerics as the exact solution. However, for the case when $\beta = \infty$ which corresponds to the inviscid case gives the correct answer when comparing with the exact solution. Also, it is the same result for the inviscid case in previous findings by Sader [15] for the normal oscillations as well as Green and Sader [7] for the torsional case.

In the Fig. 5.1, we see that the solution obtained from the Wiener-Hopf method has a constant slope on the log-log plot. But in all cases except $Im(\Gamma^t(\beta))$, we see that the slope decreases a bit as we increase the Reynolds number. This indicates that there are higher order terms influencing the results, causing it to decrease the slope but ever so slightly. In the case

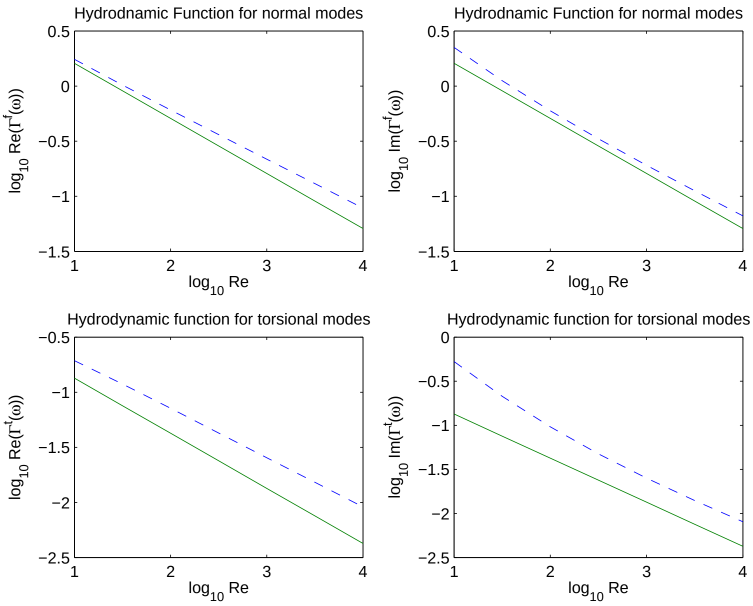

Figure 5.1: The real and imaginary parts of $\Gamma^n(\beta)$ and $\Gamma^t(\beta)$ excluding the inviscid part on a log-log plot. The solid lines are the solutions obtained from the Wiener-Hopf method while the dashed lines are the exact solutions

of $Im(\Gamma^t(\beta))$, the slope seem to approach a constant value which might indicate that the higher order terms in the other cases is not affecting this one.

We perform a further check on whether the exact solution follows the behaviour of the results from the Wiener-Hopf method, namely that the hydrodynamic function is inversely proportional to the $\sqrt{\beta}$. If it fails, then it might mean that there is a higher order term which is non-negligible that needs to be included in the results of the Wiener-Hopf method. From Fig. 5.2, the exact solution doesn't seem to be following the trend that it is inversely proportional to $\sqrt{\beta}$ since it does not trace a straight line at -0.5 on the vertical axis. Moreover, it does not seem to follow any pure power of the Reynolds number which does suggest higher order terms are at play.

From the hydrodynamic function obtained for the case of normal oscil-

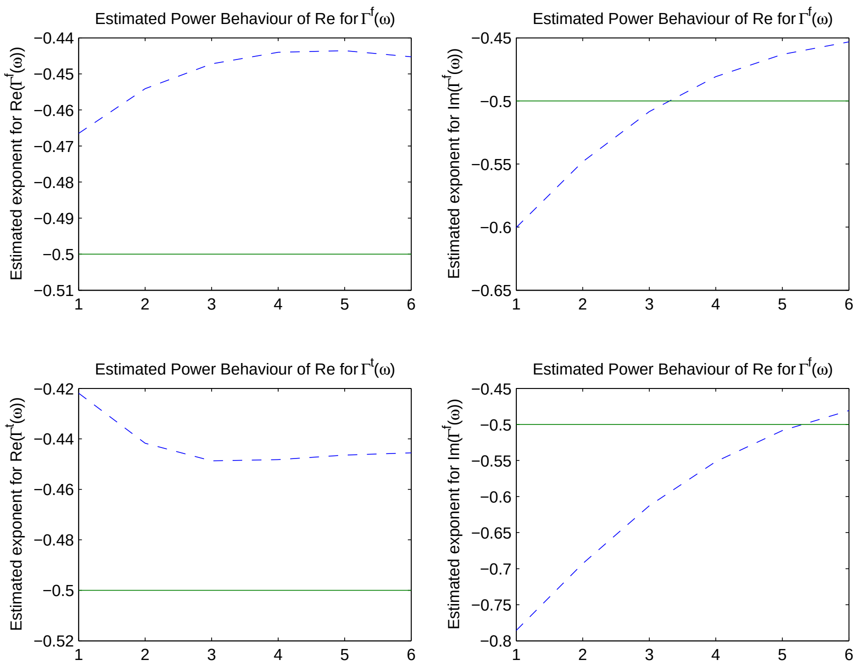

Figure 5.2: Estimated power law behaviour for the solutions. The solid lines are the solutions from the Wiener-Hopf method and the dashed lines are the exact solutions. A straight line indicates a power law behaviour in β

lations, we can compare the damping coefficient obtained here with that of Tuck's. However, the Reynolds number used by Tuck differs by a factor 4 in the denominator. So, in order to make our result comparable with Tuck, we need to replace $\sqrt{\beta}$ with $2\sqrt{\beta}$ in the hydrodynamic function. To get the damping coefficient, one needs to take the imaginary part of the hydrodynamic function since it corresponds to the drag force:

$$\begin{aligned} Im(\Gamma^n(\beta)) &= \frac{8\sqrt{2}}{\pi}\sin(\frac{\pi}{4}) \\ &= \frac{8}{\pi} \\ &\approx 2.55 \quad . \end{aligned}$$

The damping coefficient also falls short of the result by Tuck which again suggest some terms which are significant are not accounted for in the Wiener-Hopf method.

One explanation as to why there may be some neglected terms in the Wiener-Hopf solution is primarily due to the edges. The method used to solve for the fluid flow is to calculate the potential flow first and then using the information about the potential flow, a correction was obtained to include viscous effects. In literature, this is seen as the leading order term in a matched asymptotic expansion between the outer region where the fluid is governed by the Euler equation concerning inviscid flow and the inner region where viscous effect takes place. For an infinite plate oscillating, the outer region consist of a fluid that has zero vorticity due to the canceling of positive and negative vorticity when oscillating [10]. Hence, it obeys the governing equation for an inviscid fluid. But there is a thin layer where vorticity is non-zero which is the region where viscous effects have penetrated the fluid. For an infinite plate, the thin boundary layer is present throughout the entire plate and has a length scale

$$\delta \sim \sqrt{\frac{\mu}{\omega\rho}}$$

But, for a plate that has an edge, the fluid around the region of the edge "sees" the plate as infinite in one direction and thus we have no natural length scale. If we define a local Reynolds number about the edge

$$\beta_y = \frac{y^2\rho\omega}{\mu}$$

where y is the distance from the edge and the corresponding length scale

$$\delta(y) \sim y\sqrt{\frac{\mu}{\omega\rho}}$$

we see that if we get closer to the edge, the local Reynolds number becomes small and thus the fluid will be governed by Stokes flow. This means that the assumption of a thin boundary layer breaks down near the edges because the viscous penetration depth far away from the edges are considered large compared to the distance from the edge. So, we expect another contribution from the edge apart from the viscous effect due to the thin boundary layer far away from the edge that needs to be included in our solution.

We also expect higher order terms which do not follow a pure power behaviour but also possibly logarithmic terms. Performing a regular perturbation expansion for small β shows that the solution does not satisfy the condition that the fluid is stationary far away from the plate. This is commonly known in literature as Stokes paradox. For a 2-D fluid flow, it can be shown that the solution diverges logarithmically as we move off to infinity from the edge. To correct for this, we necessarily need to have logarithmic

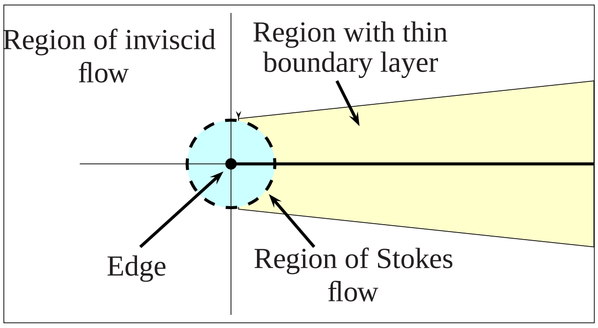

Figure 5.3: Regions of inviscid flow, Stokes flow and thin boundary layers occur with respect to an edge of a blade

terms in the expansion and subsequently in the additional contribution to the solution. Further evidence of a logarithmic type behaviour comes from the asymptotics of the hydrodynamic function calculated by Sader for normal oscillations and by Green and Sader for torsional oscillations. As $\beta \to 0$, the function behaves as

$$\Gamma^n(\beta) \sim -\frac{4i}{\beta \ln(-i\sqrt{i\beta})}$$
$$\Gamma^t(\beta) \sim \frac{i}{\beta} - \frac{3}{8}\ln(-i\sqrt{i\beta})$$

as $\beta \to 0$. So if we approach the edge, the hydrodynamic function should be able to pick up the same behaviour as quoted above. Therefore we must have logarithmic terms in the hydrodynamic function to be able to capture this.

From the expressions of Γ^n and Γ^t above, it is interesting to note that Stokes paradox doesn't occur for the $Im(\Gamma^t)$ since $Im(\beta\Gamma^t)$ does not have anymore terms involving β where length scales are present. This links with the results in the corresponding figure which seem to approach a constant slope and so we might not expect to have higher order terms corresponding to the existence of Stokes paradox for this case.

To properly account for the behaviour at the edges, one must do a matched asymptotic expansion to match the region of inviscid flow with the region with boundary layers and at the same time, match it with the region near the edges (see Fig. 5.3). This has been suggested by Rosenhead [14] and has been done for a few cases like flow past a sphere, a cylinder and a flat plate with one edge albeit for $\beta \to 0$. So, any problem that has an edge in it requires one to go through these 3 steps to get the leading order behaviour. The approach taken from Atkinson and de Lara has only completed 2 of the 3 steps mentioned above and from our results, it seems that the third and final step is also crucial to complete the analysis. In their original paper, their problem is a wide clamped plate that has a free edge. It is likely that this edge would need to be accounted for to give accurate results as well which they have not done. The problem of the vibrating disk that they have studied also have an edge and we might need to correct for the edges.

Chapter 6

Conclusions

In this thesis, the main aim was to understand the Wiener-Hopf method and its application to solve the fluid flow problems of an infinite nature. The problem studied by Atkinson and de Lara where the method was first applied was for an infinitely wide flat plate clamped on one end and free to vibrate on the other end. The method was applied to obtain the correction to the inviscid solution for the pressure differential and the force exerted on the plate was calculated. The fluid force is coupled with the equation of motion for a thin plate. Numerous typographical errors and some minor inconsistencies were encountered. In particular, the use of Green's function to solve for the equation of motion of the plate was not appropriate. Instead, the method of eigenfunction expansions was used.

The Wiener-Hopf method has been utilized to solve similiar vibrational problems to which the exact solution has been obtained by Van Eysden and Sader. The goal is to extract asymptotics for large Reynolds number using this method and to compare it with the numerics from the exact solution. The method is not able to capture the full behaviour in the cases of normal and torsional oscillations. The assumption that at the region near the edges of the blade, the correction behaves as $1/\sqrt{\beta}$ has been suggested as the main culprit. This is because the boundary layer at the edges are no longer thin to allow a square root behaviour. It is very likely that it is because of failure of thin boundary layers at the edges that may give a non-negligible, higher order contributions to the asymptotics.

This draws doubt on the validity of the solution obtained by Atkinson and de Lara for the wide clamped plate. The plate still have an edge in the problem and it is likely that the solution would not be able to accurately capture the true underlying behaviour. The authors have failed to realise that they haved modeled this problem as a pure 2-D flow with an edge and thus will need to worry about Stokes' paradox at the edge. Nevertheless, their method was able to give a first approximation to the viscous effects to correct for the inviscid flow. This has the behaviour for the high Reynolds number for regions sufficiently far away from the edges primarily around the origin. The same problem would also arise since they have also solved the case of a vibrating disk which has a circular edge as well.

6.1 Future research

An area for future research is to perform the final part of the matched asymptotic expansion for the problem as suggested by Rosenhead. That is, to match the solution obtained in this thesis with the region near the edge where it is governed by Stokes flow to obtain the term in the leading order behaviour.

Appendix A

Product Decomposition of $H(\zeta)$

We have that the function $H(\zeta)$ can be decomposed into plus and minus functions in terms of integrals over the real axis:

$$\ln\left(H_{+}(\zeta)\right) = \frac{1}{2\pi i}\int_{-\infty}^{\infty}\frac{\ln(H(z))}{z-\zeta}\mathrm{d}z, \quad Im(\zeta) > 0 \tag{A.1a}$$

$$\ln\left(H_{-}(\zeta)\right) = -\frac{1}{2\pi i}\int_{-\infty}^{\infty}\frac{\ln(H(z))}{z-\zeta}\mathrm{d}z \quad Im(\zeta) < 0 \quad . \tag{A.1b}$$

where $H(\zeta)$ is defined as

$$H(\zeta) = \frac{\sqrt{\zeta}_{+}\sqrt{\zeta}_{-} + \sqrt{\zeta^2 - i}}{2\sqrt{\zeta^2 - i}}$$

and $\sqrt{\zeta}_{+}$ and $\sqrt{\zeta}_{-}$ are defined in (3.32).

A.1 Large ζ expansion of $H_+(\zeta)$

Consider the integral

$$\oint_{\Gamma_1} \frac{\ln(H(z))}{z-\zeta} \mathrm{d}z \quad .$$

There are branch points at $\pm i\delta$ and $\pm e^{-i\pi/4}$ corresponding to the functions $\sqrt{\zeta_+}\sqrt{\zeta_-}$ and $\sqrt{\zeta^2 - i}$ respectively. There are no zeros for the function $H(\zeta)$ hence there are no branch points for the logarithm. So we choose the branch cuts such that they join between $i\delta$ and $e^{-i\pi/4}$ together and similiarly between $-i\delta$ and $-e^{i\pi/4}$. For the upper branch cut, the square root function will take the positive square root and for the lower branch cut, the negative square root will be taken. The contour Γ_1 is chosen to go along the real axis and closing in the lower half plane. This is because $H_+(\zeta)$ is analytic in the upper half plane meaning that $Im(\zeta) > 0$ and so we have a pole in the upper half plane with $z = \zeta$.

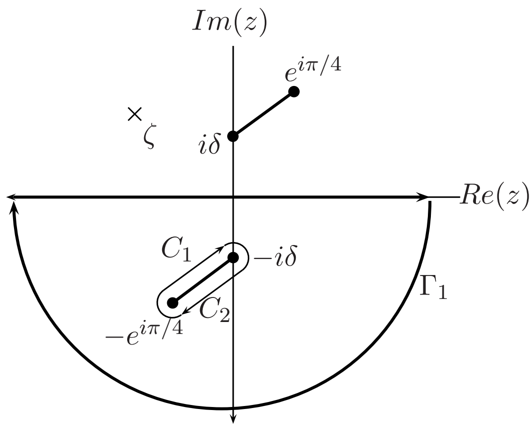

Figure A.1: Contour used for simplifying $H_+(\zeta)$

Because there are no poles but just a branch cut in the lower half plane, we can analytically deform the contour Γ_1 until we enclose the branch cut in the lower half plane. The contribution from the semicircle, C_R, is zero since we have that $H(\zeta) \to 1$ and therefore $\ln(H(\zeta)) \to 0$ as $|\zeta| \to \infty$. The contribution from circling the branch points can be shown to be zero. So, we have

$$\oint_{\Gamma} \frac{\ln(H(z))}{z-\zeta} \mathrm{d}z = \int_{C_1+C_2} \frac{\ln(H(z))}{z-\zeta} \mathrm{d}z \quad . \tag{A.2}$$

We can take the limit as $\delta \to 0$ and the RHS of the equation reduces to

$$\begin{aligned} &\int_{C_1+C_2} \ln\left(\frac{1}{2}\sqrt{\frac{z^2}{z^2-i}} + \frac{1}{2}\right) \frac{1}{z-\zeta} \mathrm{d}z \\ &= \int_0^{-e^{i\pi/4}} \ln\left(\frac{iz}{2\sqrt{i-z^2}} + \frac{1}{2}\right) \frac{1}{z-\zeta} \mathrm{d}z \\ &\quad - \int_0^{-e^{i\pi/4}} \ln\left(\frac{-iz}{2\sqrt{z^2-i}} + \frac{1}{2}\right) \frac{1}{z-\zeta} \mathrm{d}z \quad . \end{aligned} \tag{A.3}$$

Performing a change of variables $z = -re^{i\pi/4}$ and with the branch cut having the argument $-3\pi/4 < \arg(z) < 5\pi/4$, we have

$$\begin{aligned} &\int_0^1 \ln\left(\frac{-ire^{i\pi/4} + e^{i\pi/4}\sqrt{1-r^2}}{2e^{i\pi/4}\sqrt{1-r^2}}\right) \frac{e^{i\pi/4}}{re^{i\pi/4}+\zeta} \mathrm{d}r \\ &\quad - \int_0^1 \ln\left(\frac{re^{i\pi/4} + e^{i\pi/4}\sqrt{1-r^2}}{2e^{i\pi/4}\sqrt{1-r^2}}\right) \frac{e^{i\pi/4}}{re^{i\pi/4}+\zeta} \mathrm{d}r \\ &= \int_0^1 \ln\left(\frac{-ir + \sqrt{1-r^2}}{2\sqrt{1-r^2}}\right) \frac{e^{i\pi/4}}{re^{i\pi/4}+\zeta} \mathrm{d}r \\ &\quad - \int_0^1 \ln\left(\frac{ir + \sqrt{1-r^2}}{2\sqrt{1-r^2}}\right) \frac{e^{i\pi/4}}{re^{i\pi/4}+\zeta} \mathrm{d}r \\ &= \int_0^1 \frac{e^{i\pi/4}\ln(-ir+\sqrt{1-r^2})}{re^{i\pi/4}+\zeta} \mathrm{d}r \\ &\quad - \int_0^1 \frac{e^{i\pi/4}\ln(ir+\sqrt{1-r^2})}{re^{i\pi/4}+\zeta} \mathrm{d}r \\ &= -2ie^{i\pi/4} \int_0^1 \frac{\arcsin(r)}{re^{i\pi/4}+\zeta} \mathrm{d}z \quad , \end{aligned} \tag{A.4}$$

where from the second to the third line we can cancel the denominator in the logarithms since they are no longer multivalued in the domain on integration and from the third to the last line, we used the identity that

$i\arcsin(z) = \ln(iz + \sqrt{1-z^2})$. Going back to the integral in (A.2), we have that

$$\oint_{\Gamma} \frac{\ln(H(z))}{z-\zeta}\mathrm{d}z = -2ie^{i\pi/4}\int_0^1 \frac{\arcsin(r)}{re^{i\pi/4}+\zeta}\mathrm{d}z$$
$$\int_{-\infty}^{\infty} \frac{\ln(H(z))}{z-\zeta}\mathrm{d}z = -2ie^{i\pi/4}\int_0^1 \frac{\arcsin(r)}{re^{i\pi/4}+\zeta}\mathrm{d}z \quad .$$

Substituting the expression for the integral above into (A.1a), we have

$$\ln(H_+(\zeta)) = -\frac{e^{i\pi/4}}{\pi}\int_0^1 \frac{\arcsin(r)}{re^{i\pi/4}+\zeta}\mathrm{d}z \quad . \tag{A.5}$$

Expanding for $|\zeta| \to \infty$ we get

$$\begin{aligned} \ln(H_+(\zeta)) &= -\frac{e^{i\pi/4}}{\pi\zeta}\int_0^1 \arcsin(r)\mathrm{d}z + O\left(\frac{1}{\zeta^2}\right) \\ \Rightarrow \qquad H_+(\zeta)|_{|\zeta|\to\infty} &\approx \exp\left(-\frac{\pi-2}{2\pi}\frac{e^{i\pi/4}}{\zeta}\right) \\ &\approx 1 - \frac{\pi-2}{2\pi}\frac{e^{i\pi/4}}{\zeta} + \cdots \end{aligned} \tag{A.6}$$

A.2 Large ζ expansion of $H_-(\zeta)$

We still consider the same contour integral in the previous section except with the contour Γ_2 but all its properties are the same since for $H_-(\zeta)$ to be analytic in the lower half plane, there is a pole in that region. So, we still have the same form as (A.2) except that the contours would be enclosing the upper branch cut:

$$\oint_{\Gamma_2} \frac{\ln(H(z))}{z-\zeta}\mathrm{d}z = \int_{C_1+C_2} \frac{\ln(H(z))}{z-\zeta}\mathrm{d}z \quad . \tag{A.7}$$

Taking $\delta \to 0$, performing a change of variables $z = re^{i\pi/4}$ and noting that the argument of the branch cut is $-7\pi/4 < \arg(z) < \pi/4$ and following

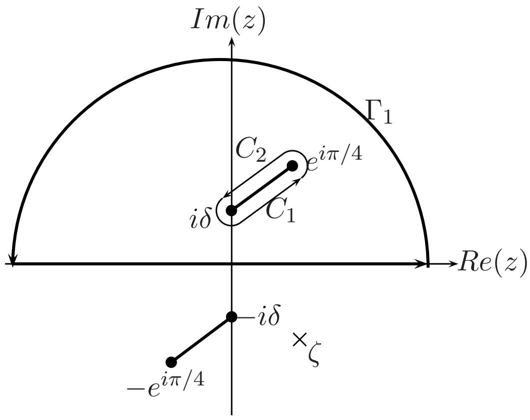

Figure A.2: Contour for simplifying $H_-(\zeta)$

the same arguments as before, we get the RHS of (A.7) to be

$$2ie^{i\pi/4}\int_0^1 \frac{\arcsin(r)}{re^{i\pi/4}-\zeta}\mathrm{d}r \quad .$$

Substituting the above equation in (A.7) and substituting the result into (A.1b), we have

$$\ln\left(H_-(\zeta)\right) = -\frac{e^{i\pi/4}}{\pi}\int_0^1 \frac{\arcsin(r)}{re^{i\pi/4}-\zeta}\mathrm{d}r \quad . \tag{A.8}$$

Expanding for $|\zeta| \to \infty$

$$\begin{aligned} \ln\left(H_-(\zeta)\right) &= \frac{e^{i\pi/4}}{\pi\zeta}\int_0^1 \arcsin(r)\mathrm{d}r + O\left(\frac{1}{\zeta^2}\right) \\ \Rightarrow \quad H_-(\zeta)|_{|\zeta|\to\infty} &\approx \exp\left(\frac{\pi-2}{2\pi}\frac{e^{i\pi/4}}{\zeta}\right) \\ &\approx 1 + \frac{\pi-2}{2\pi}\frac{e^{i\pi/4}}{\zeta} + \cdots \end{aligned} \tag{A.9}$$

Appendix B

Sum decomposition of $S(\zeta)$

We have the function $S(\zeta)$ that can be decomposed to $S_+(\zeta)$ and $S_-(\zeta)$ to be

$$S_+(\zeta) = \frac{1}{2\pi i}\int_{-\infty}^{\infty}\frac{S(z)}{z-\zeta}\mathrm{d}z \quad Im(\zeta) > 0 \tag{B.1a}$$

$$S_-(\zeta) = -\frac{1}{2\pi i}\int_{-\infty}^{\infty}\frac{S(z)}{z-\zeta}\mathrm{d}z \quad Im(\zeta) < 0 \quad , \tag{B.1b}$$

where

$$S(\zeta) = \left[\frac{\sqrt{\zeta}_-}{\sqrt{\zeta}_+}\sqrt{\frac{\zeta + e^{i\pi/4}}{\zeta - e^{i\pi/4}}} - 1\right] H_+(\zeta) \quad .$$

B.1 Large ζ expansion of $S_-(\zeta)$

We consider the contour integral

$$\begin{aligned}
&\oint_{\Gamma_1}\frac{S(z)}{z-\zeta}\mathrm{d}z \\
&= \oint_{\Gamma_1}\frac{\sqrt{z}_-}{\sqrt{z}_+}\sqrt{\frac{z+e^{i\pi/4}}{z-e^{i\pi/4}}}\frac{H_+(z)}{z-\zeta}\mathrm{d}z - \oint_{\Gamma_1}\frac{H_+(z)}{z-\zeta}\mathrm{d}z \\
&= \oint_{\Gamma_1}\frac{\sqrt{z}_-}{\sqrt{z}_+}\sqrt{\frac{z+e^{i\pi/4}}{z-e^{i\pi/4}}}\frac{H_+(z)}{z-\zeta}\mathrm{d}z
\end{aligned}$$

since $S_-(\zeta)$ is analytic in the lower half plane, so there is a pole in the lower half plane with $z = \zeta$. Because the contour Γ_1 goes along the real axis and closes in the upper half plane and $H_+(\zeta)$ is analytic in the upper half plane, the second integral vanishes by Cauchy's theorem. The branch points and the contour is the same as in Fig. A.2 in Appendix A.2. The contribution of the semi circle goes to zero since we have $S(\zeta) \to 0$ as $|\zeta| \to \infty$. So,

$$\oint_{\Gamma_1} \frac{\sqrt{z_-}}{\sqrt{z_+}} \sqrt{\frac{z + e^{i\pi/4}}{z - e^{i\pi/4}}} \frac{H_+(z)}{z - \zeta} \mathrm{d}z = \int_{C_1+C_2} \frac{\sqrt{z_-}}{\sqrt{z_+}} \sqrt{\frac{z + e^{i\pi/4}}{z - e^{i\pi/4}}} \frac{H_+(z)}{z - \zeta} \mathrm{d}z \quad . \tag{B.2}$$

Taking $\delta \to 0$ and noting that the argument of the branch cut is $-7\pi/4 < \arg(z) < \pi/4$, the RHS of the equation now becomes

$$2i \int_0^{e^{i\pi/4}} \sqrt{\frac{z + e^{i\pi/4}}{e^{i\pi/4} - z}} \frac{H_+(z)}{z - \zeta} \mathrm{d}z.$$

Performing a change of variables $z = re^{i\pi/4}$, this becomes

$$2ie^{i\pi/4} \int_0^1 \sqrt{\frac{1 + r}{1 - r}} \frac{H_+(re^{i\pi/4})}{re^{i\pi/4} - \zeta} \mathrm{d}r \tag{B.3}$$

Substituting (B.3) into (B.2) we get

$$\int_{-\infty}^{\infty} \frac{S(z)}{z - \zeta} \mathrm{d}z = 2ie^{i\pi/4} \int_0^1 \sqrt{\frac{1 + r}{1 - r}} \frac{H_+(re^{i\pi/4})}{re^{i\pi/4} - \zeta} \mathrm{d}r \quad . \tag{B.4}$$

Substituting the equation above into (B.1b),

$$S_-(\zeta) = -\frac{e^{i\pi/4}}{\pi} \int_0^1 \sqrt{\frac{1 + r}{1 - r}} \frac{H_+(re^{i\pi/4})}{re^{i\pi/4} - \zeta} \mathrm{d}r \quad , \tag{B.5}$$

where

$$H_+(re^{i\pi/4}) = \exp\left(-\frac{1}{\pi} \int_0^1 \frac{\arcsin(r')}{r' + r} \mathrm{d}r'\right) \quad .$$

Expanding for $|\zeta| \to \infty$ for (B.5)

$$S_-(\zeta)|_{|\zeta|\to\infty} = \frac{e^{i\pi/4}}{\pi\zeta}\int_0^1 \sqrt{\frac{1+r}{1-r}}H_+(re^{i\pi/4})\mathrm{d}r + \frac{i}{\pi\zeta^2}\int_0^1 r\sqrt{\frac{1+r}{1-r}}H_+(re^{i\pi/4})\mathrm{d}r + O\left(\frac{1}{\zeta^3}\right) \quad .$$

Atkinson and de Lara have claimed that the following integrals give

$$\begin{aligned}\int_0^1 \sqrt{\frac{1+r}{1-r}}H_+(re^{i\pi/4})\mathrm{d}r &= \frac{\pi}{\sqrt{2}} \quad , \\ \int_0^1 r\sqrt{\frac{1+r}{1-r}}H_+(re^{i\pi/4})\mathrm{d}r &= \frac{\pi}{2} \quad .\end{aligned} \tag{B.6}$$

It is not certain how they have evaluated these rather difficult integrals. Nonetheless, numerical integration has shown both to be accurate to 8 decimal places. In the analysis, we use the values of the integrals as above since this greatly simplifies the asymptotics.

B.2 Large ζ expansion of $S_+(\zeta)$

By using the usual method for simplifying $S_-(\zeta)$, we will have to evaluate more complicated integrals. But since we are interested in the expansion of the function as $|\zeta| \to \infty$, we just subtract the expansion for $S_+(\zeta)$ from the expansion of $S(\zeta)$ for large ζ. The expansion for $S(\zeta)$ for large ζ is calculated to be

$$S(\zeta)|_{|\zeta|\to\infty} = \frac{e^{i\pi/4}}{\zeta} + \frac{i}{\pi\zeta^2} + \cdots$$

Therefore, $S_+(\zeta)$ is found to be

$$\begin{aligned}S_+(\zeta)|_{|\zeta|\to\infty} &= S(\zeta) - S_-(\zeta) \\ &= e^{i\pi/4}\left(1 - \frac{1}{\sqrt{2}}\right)\frac{1}{\zeta} + i\left(\frac{1}{\pi} - \frac{1}{2}\right)\frac{1}{\zeta^2} \quad .\end{aligned} \tag{B.7}$$

Appendix C

Contour integrals

The main method that is being used here is calculating the residue at infinity.

The way this is calculated is

$$Res(f(z))|_{z=\infty} = \lim_{z\to\infty} zf(z)$$

With this, we can make use of Cauchy residue theorem.

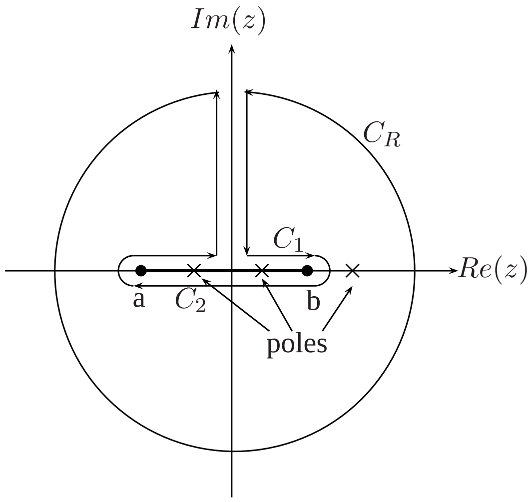

Figure C.1: Contours for all integrals here. The contribution going from the cut to C_R cancel each other and the distance apart can be made arbitrarily small

In all the integrals considered here in this thesis, there will be 2 branch points on the real axis and the branch cut is chosen to join the two points through the origin. Also, we will have poles on the cut and may have poles outside as well. Because the branch cut is due to a square root function, the contribution from traversing along an arbitrarily small semicircle around the pole on the upper cut will cancel the contribution from traversing along an arbitrarily small semicircle around the pole on the lower cut. Contributions from circling the branch points are also shown to be zero. So, with the contour given in the Fig. C.1, the only things that matter are poles outside the branch cut and the contour integral C_R.

$$\begin{aligned}
\int_{C_1+C_2} f(z)\mathrm{d}z &= 2\pi i \sum Res(f(z)) - \int_{C_R} f(z)\mathrm{d}z \\
2i\int_{C_1} g(z)\mathrm{d}z &= \pi i \left[\sum Res(f(z)) + Res(f(z))_{z\to\infty}\right] \\
\int_a^b g(z)\mathrm{d}z &= \pi \left[\sum Res(f(z)) + \lim_{z\to\infty} z f(z)\right] \qquad \text{(C.1)}
\end{aligned}$$

since travelling along the top cut we can take out a factor of (-1) from the square root in $f(z)$ and it will take the value $ig(z)$ while along the bottom cut, it will take the value $-ig(z)$. The minus sign is removed in the second line is due to the orientation of the contour C_R with respect to the point at infinity.

C.1 Integral in Equation (3.18)

We have the functions

$$\begin{aligned}
f(z) &= \frac{1}{(y-z)(y'-z)}\sqrt{\frac{z}{z-1}} \quad , \\
g(z) &= \frac{1}{(y-z)(y'-z)}\sqrt{\frac{z}{1-z}} \quad ,
\end{aligned}$$

where there is a pole outside the cut at $z = y > 1$ and a pole at $0 < z = y' < 1$ in the cut. We have that

$$\begin{aligned}\lim_{|z|\to\infty} zf(z) &= \lim_{|z|\to\infty} \frac{z}{(y-z)(y'-z)}\sqrt{\frac{z}{z-1}} \\ &= 0 \quad .\end{aligned}$$

Therefore the contour integral in (C.1) now becomes

$$\int_0^1 \frac{1}{(y-s)(y'-s)}\sqrt{\frac{s}{1-s}}\mathrm{d}s = \pi\left(\frac{1}{y'-y}\sqrt{\frac{y}{1-y}}\right) \quad .$$

C.2 Integral in Equation (3.37)

The functions in the equation are

$$\begin{aligned}f(z) &= \frac{1}{y'-z}\sqrt{\frac{z}{z-1}} \quad , \\ g(z) &= \frac{1}{y'-z}\sqrt{\frac{z}{1-z}} \quad ,\end{aligned}$$

where we only have a pole at $0 < z = y' < 1$. We have that

$$\begin{aligned}\lim_{|z|\to\infty} zf(z) &= \lim_{|z|\to\infty} \frac{z}{y'-z}\sqrt{\frac{z}{z-1}} \\ &= -1 \quad .\end{aligned}$$

Therefore the contour integral becomes

$$\int_0^1 \frac{1}{y'-z}\sqrt{\frac{z}{1-z}}\mathrm{d}z = -\pi \quad .$$

C.3 Integral in Equation (4.14)

The functions are

$$f(z) = \frac{z}{\sqrt{4z^2-1}}\frac{1}{(y'^2-z^2)(y-z)} \quad ,$$
$$g(z) = \frac{z}{\sqrt{1-4z^2}}\frac{1}{(y'^2-z^2)(y-z)} \quad .$$

There are poles at $z = \pm y'$ on the cut where $-1/2 < y' < 1/2$ and a pole at $z = y > 1$. The branch points are $\pm 1/2$. We have that

$$\begin{aligned}\lim_{|z|\to\infty} zf(z) &= \lim_{|z|\to\infty} \frac{z^2}{\sqrt{4z^2-1}}\frac{1}{(y'^2-z^2)(y-z)} \\ &= 0 \quad .\end{aligned}$$

The contour integral now becomes

$$\begin{aligned}\int_{-1/2}^{1/2} \frac{s}{\sqrt{1-4s^2}}\frac{1}{(y'^2-s^2)(y-s)}\mathrm{d}s &= \pi i Res(f(z))|_{z=y} \\ &= \pi i\left(\frac{y}{\sqrt{4y^2-1}}\frac{1}{y'^2-y^2}\right) \quad .\end{aligned}$$

C.4 Integral in Equation (4.19) and (4.32)

The functions are

$$f(z) = \frac{z^2}{\sqrt{4z^2-1}}\frac{1}{y'^2-z^2}\mathrm{d}z \quad ,$$
$$g(z) = \frac{z^2}{\sqrt{1-4z^2}}\frac{1}{y'^2-z^2}\mathrm{d}z \quad .$$

We have poles at $\pm y'$ which is on the cut and no poles outside. We have that

$$
\begin{aligned}
\lim_{|z|\to\infty} zf(z) &= \lim_{|z|\to\infty} \frac{z^3}{\sqrt{4z^2-1}}\frac{1}{y'^2-z^2}\mathrm{d}z \\
&= -\frac{1}{2} \quad .
\end{aligned}
$$

The contour integral now reduces to

$$
\int_{-1/2}^{1/2} \frac{s^2}{\sqrt{1-4s^2}}\frac{1}{y'^2-s^2}\mathrm{d}s = -\frac{\pi}{2} \quad .
$$

C.5 Integral in Equation (4.25)

The functions are

$$
\begin{aligned}
f(z) &= \frac{1}{\sqrt{4z^2-1}}\frac{1}{y'^2-z^2} \quad , \\
g(z) &= \frac{1}{\sqrt{1-4z^2}}\frac{1}{y'^2-z^2} \quad .
\end{aligned}
$$

There are poles at $\pm y'$ on the cut but none outside. We have that

$$
\lim_{|z|\to\infty} f(z) = 0 \quad ,
$$

therefore, the contour integral is trivial, that is

$$
\int_{-1/2}^{1/2} \frac{1}{\sqrt{1-4s^2}}\frac{1}{y'^2-s^2}\mathrm{d}s = 0 \quad .
$$

C.6 Integral in Equation (4.29)

Similiar to the previous section but now $f(z)$ has a pole at $z = y > 1$ outside the cut:

$$\begin{aligned} f(z) &= \frac{1}{\sqrt{4z^2-1}} \frac{1}{(y'^2 - z^2)(y-z)} \quad , \\ g(z) &= \frac{1}{\sqrt{1-4z^2}} \frac{1}{(y'^2 - z^2)(y-z)} \quad . \end{aligned}$$

So the integral becomes

$$\begin{aligned} \int_{-1/2}^{1/2} \frac{1}{\sqrt{1-4s^2}} \frac{1}{(y'^2 - s^2)(y-s)} \mathrm{d}s &= \pi i Res(f(z))|_{z=y} \\ &= \pi i \left(\frac{1}{\sqrt{4y^2-1}} \frac{1}{y'^2 - y^2} \right) \quad . \end{aligned}$$

Bibliography

[1] M. J. Ablowitz and A. S Fokas. *Complex Variables: Introduction and applications*. Cambridge University Press, 2003.

[2] C. Atkinson and M. M. de Lara. Fluid reaction on a vibrating disc in a viscous medium. *International Journal of Engineering Science*, 44:973–995, 2006.

[3] C. Atkinson and M. M. de Lara. The frequency response of a rectangular cantilever plate vibrating in a viscous fluid. *Journal of Sound and Vibration*, 300:352–367, 2007.

[4] G. K. Batchelor. *Introduction to Fluid Dynamics*. Cambridge University Press, 1974.

[5] C. A. Van Eysden and J. E. Sader. Small amplitude oscillations of a flexible thin blade in a viscous fluid: Exact analytical solution. *Physics of Fluids*, 18, 2006.

[6] C. A. Van Eysden and J. E. Sader. Frequency response of cantilever beams immersed in viscous fluids with applications to the atomic force microscope: Arbitrary mode order. *Journal of Applied Physics*, 101, 2007.

[7] C. P. Green and J. E. Sader. Torsional frequency response of cantilever beams immersed in viscous fluids with applications to the atomic force microscope. *Journal of Applied Physics*, 92:6262–6274, 2002.

[8] J. R. Hanna. *Fourier series and integrals of boundary value problems.* Wiley Interscience, New York, 1982.

[9] G. M. Kapoulitsas. Scattering of long waves in a rotating bifurcated channel. *International Journal of Theoretical Physics*, 19, 1980.

[10] L. D. Landau and E. M. Lifshitz. *Fluid Mechanics.* Pergamon Press, 2nd edition, 1987.

[11] M. Masujima. *Applied Mathematical Methods in Theoretical Physics.* Wiley-VCH Verlag GmbH & Co. KGaA, 2005.

[12] N. I. Muskhelishvili. *Singular Integral Equations.* Noordhoff, Groningen, 1953.

[13] B. Noble. *Methods based on the Wiener-Hopf technique for the solution of partial differential equations.* Pergamon Press, 1958.

[14] L. Rosenhead. *Laminar Boundary Layers.* Clarendon, Oxford University Press, 1963.

[15] J.E Sader. Frequency response of cantilever beams immersed in viscous fluids with applications to the atomic force microscope. *Journal of Applied Physics*, 84:64–76, 1998.

[16] S. P. Timoshenko and S. Woinowsky-Kreiger. *Theory of Plates and Shells.* McGraw-Hill, New York, 1959.

[17] E. O. Tuck. Calculation of unsteady flows due to small motions of cylinders in a viscous fluid. *Journal of Engineering Mathematics*, 3:29–44, 1969.